https://doi.org/10.5194/bg-2023-127
Preprint. Discussion started: 21 August 2023

Biogeosciences Discussions

Zooplankton as the primary diet for cold-water scleractinian corals (CWCs): implications for the CWC marine N cycle proxy and trophic ecology.

Josie L. Mottram[1], Anne M. Gothmann[2], Maria G. Prokopenko[3], Austin Cordova[3], Veronica Rollinson[1], Katie Dobkowski[4], Julie Granger[1]

[1]Department of Marine Sciences, University of Connecticut, Storrs, CT, 06340, USA
[2]Departments of Physics and Environmental Studies, St. Olaf College, Northfield, MN, 55057, USA
[3]Department of Geology, Pomona College, Claremont, CA, 91711, USA
[4]Department of Environmental Studies, Woodbury University, Burbank, CA, 91504, USA

Correspondence to: Anne M. Gothmann (gothma1@stolaf.edu)

Abstract. The nitrogen (N) isotope composition ($\delta^{15}N$) of cold-water corals is a promising proxy for reconstructing past ocean N cycling, as a strong correlation was found between the $\delta^{15}N$ of the organic nitrogen preserved in coral skeletons and the $\delta^{15}N$ of sinking particulate organic matter exported from the surface ocean. However, a large offset of 8-9 ‰ between the $\delta^{15}N$ recorded by the coral and that of export remains unexplained. The 8-9 ‰ offset may signal a potential sensitivity of the proxy to food web structure, an unusual large trophic isotope effect or a biosynthetic $\delta^{15}N$ offset between the coral's soft tissue and skeletal tissues, or some combinations of these factors. To understand the origin of the offset and further validate the proxy, we investigated the trophic ecology of the scleractinan cold water coral *Balanophyllia elegans*. A long-term incubation experiment of *B. elegans* fed on an isotopically controlled diet yielded a canonical trophic isotope effect of 3.0 ± 0.1‰ between coral soft tissue and the *Artemia* prey. The trophic isotope effect was not detectably influenced by sustained food limitation. A long N turnover of coral soft tissue of 291 ± 15 days in the well-fed incubations indicates that the coral skeleton is not apt to record seasonal difference in diet $\delta^{15}N$. Specimens of *B. elegans* from the shallow subtidal zone near San Juan Channel (WA, USA) revealed a modest difference between soft and skeletal tissue $\delta^{15}N$ of 1.2 ± 0.6 ‰. The $\delta^{15}N$ of the coral soft tissue was 12.0 ± 0.6 ‰, which was ~6 ‰ higher than that of suspended organic material that was comprised dominantly of phytoplankton – suggesting that the latter is not the primary component of *B. elegans'* diet. An analysis of size-fractionated net tow material suggests that *B. elegans* fed predominantly on a size class of zooplankton ≥ 500 µm, implicating a two-level trophic transfer between phytoplankton material and coral tissue. These results portend a sensitivity of cold-water coral $\delta^{15}N$ to regional food web structure that must be heeded in paleoceanographic studies of ocean N cycling.

https://doi.org/10.5194/bg-2023-127
Preprint. Discussion started: 21 August 2023


Biogeosciences Discussions Open Access EGU

30

31 ## 1 Introduction

32 Interactions between ocean circulation and nutrient cycling modulate the marine biological carbon pump
33 and the consequent partitioning of CO_2 between atmosphere and ocean, and thus influence planetary climate on
34 centennial to millennial time scales (Sigman and Boyle 2000). The marine nitrogen (N) cycle is highly sensitive
35 to these interactions, such that knowledge of modern and ancient ocean N cycling can help illuminate drivers of
36 past climate and contextualize modern global change (*e.g.*, Altabet et al., 1994; Francois et al., 1997; Robinson
37 and Sigman 2008; Sigman et al., 1999; Kast et al. 2019).

38 The main tool to investigate the oceanic N cycle history is the nitrogen (N) isotope composition (*i.e.*, the
39 $^{15}N/^{14}N$ ratio) of particulate organic nitrogen (PON) exported from the euphotic zone and preserved in various
40 paleo-archives, including bulk sedimentary N in anoxic sediments, organic N in in soft corals, and organic N
41 material preserved in foraminiferal tests and in diatom frustules (*reviewed by* Robinson et al. 2023). Henceforth,
42 we express the $^{15}N/^{14}N$ ratio in delta notation, where $\delta^{15}N$ (‰ *vs.* air) = $[[(^{15}N/^{14}N_{sample})/(^{15}N/^{14}N_{air})] - 1]*1000$.
43 The $\delta^{15}N$-PON recorded in paleo-oceanographic archives reflects both regional N cycling processes and the
44 balance of global ocean N source and sink terms (Sigman and Fripiat 2019; Brandes and Devol 2002): In regions
45 of the ocean where nitrate is quantitatively consumed, the annually integrated $\delta^{15}N$-PON exported from the
46 surface reflects the isotopic composition of thermocline nitrate (Altabet et al. 1991). The latter is influenced by
47 the circulation history of nitrate (*e.g.*, Marconi et al., 2015), by regional N_2 fixation (*e.g.*, Casciotti et al. 2008;
48 Knapp et al. 2008) and by water column denitrification (*e.g.,* Pride et al., 1999; De Pol-Holz et al., 2007). In
49 regions with incomplete consumption of surface nitrate, such as Southern Ocean, the isotopic discrimination
50 imparted during nitrate assimilation is reflected in the $\delta^{15}N$-PON, which can be used to reconstruct the degree of
51 surface nitrate consumption in the past (*e.g.,* Sigman et al., 1999; Francois et al. 1997).

52 Accurate interpretation of the N cycle's paleo-history relies on the presumption that the $\delta^{15}N$-PON preserved
53 in various palaeoceanographic archives is impervious to organic matter diagenesis. Bulk sedimentary $\delta^{15}N$
54 measurements are thus generally inadequate in this respect, subject to post-depositional processes (Robinson et
55 al. 2012) – barring fast-accumulating organic-rich anoxic sediments with negligible contribution from terrestrial
56 sources (*e.g.*, Altabet et al., 2002; Ganeshram and Pedersen, 1998). To circumvent this limitation, several
57 "biological" archives of the $\delta^{15}N$-PON have been developed that are deemed resistant to diagenetic alteration.
58 These include the organic matter intercalated in diatom frustules and foraminifera tests (*e.g.*, Ren et al., 2009;

https://doi.org/10.5194/bg-2023-127
Preprint. Discussion started: 21 August 2023

Robinson and Sigman, 2008) and the organic matter in proteinaceous corals (*e.g.*, Sherwood et al. 2009; Williams and Grottoli 2010). Recently, the $\delta^{15}N$ of organic N enclosed within the aragonite mineral lattice of asymbiotic scleractinian (stony) cold-water corals (CWCs) has been found to reflect the $\delta^{15}N$-PON exported from the surface ocean, offering an exciting new archive of marine N cycling (Wang et al. 2017; Chen et al. 2023). A robust cold-water coral archive of $\delta^{15}N$-PON can complement the existing suite of nitrogen proxies by reducing the potential biases almost inevitable for each individual proxy, allowing for a broader geographic and temporal reconstruction, and increasing resolution of the proxy record. Foremost, as with foraminifera and diatom shells, organic material trapped within the coral's original aragonite mineral lattice is presumably protected from diagenetic alteration (Drake et al. 2021); coral skeletons can be inspected for contamination and recrystallization (*e.g.*, borings) using microscopic techniques to avoid compromised areas (Gothmann et al. 2015). CWCs have a broad geographic distribution, being present in all ocean basins from the surface to 5000 m (Freiwald, 2002). They offer the potential to generate high-resolution records extending relatively far back in time, and corals have continuous skeletal accretion that records ocean conditions at the time of growth, so the analysis of multiple individuals provides enhanced temporal resolution of long-time record (Robinson et al., 2014; Hines et al. 2015). CWC skeletons are not subject to bioturbation and are thus directly dated with radiometric methods; absolute ages can be determined with decadal precision on the time scales of glacial-interglacial climate variability through U-Th series dating (Cheng et al., 2000; Goodfriend et al. 1992, Robinson et al., 2014). Remarkably, individual coral samples can archive multiple seawater properties, such that a single CWC specimen can potentially be used to reconstruct deep (*e.g.*, $\Delta^{14}C$, pH, temperature, and circulation proxies such as Ba/Ca and εNd) and surface ocean conditions ($\delta^{15}N$) at a precisely-known time (U-Th dating), making CWC unique as a paleoceanographic archive (Robinson et al., 2014; Thiagarajan et al., 2014; Rae et al. 2018).

Despite its promise, an outstanding concern about the fidelity of the $\delta^{15}N$ of coral-bound organic N is a reported 8 - 9 ‰ offset between coral-bound $\delta^{15}N$ and the corresponding $\delta^{15}N$-PON exported to regions of coral growth (Wang et al. 2014). The magnitude of this offset substantially exceeds the 3 - 3.5 ‰ expected for a single trophic transfer (Minagawa and Wada 1984), assuming that CWC feed predominantly on algal material exported from the surface ocean (Duineveld et al. 2007; 2012). Wang et al. (2014) reconciled this observation by arguing that CWCs feed on the more abundant pool of surface-derived suspended organic material (SPOM), the $\delta^{15}N$ of which is typically higher than that of sinking PON exported from the surface (Altabet 1988). While CWCs are considered generalists with regard to diet (Mortensen, 2001; Freiwald, 2002; Duineveld et al. 2004; 2007; 2012; Kiriakoulakis et al. 2005, Carlier et al., 2009, Dodds et al., 2009; van Oevelen et al. 2009), a number of studies

https://doi.org/10.5194/bg-2023-127
Preprint. Discussion started: 21 August 2023

suggest that many species of CWC subsist predominantly on metazoan zooplankton prey (Naumann et al. 2011; Kiriakoulakis et al. 2005; Carlier et al. 2009; Dodds et al. 2009; Purser et al. 2010; van Oevelen et al. 2009; Tsounis et al. 2010). A zooplankton diet should result in an approximate two-level trophic transfer between surface PON and coral tissue (*e.g.*, Sherwood et al. 2008), similar to the observed 8-9 ‰ offset and potentially rendering coral-bound $\delta^{15}N$ sensitive to spatial and temporal differences in food web structure. An alternative explanation for the offset is that there is a large biosynthetic offset between the $\delta^{15}N$ of the CWC polyp and its skeletal tissue (Horn et al. 2011; Muscatine et al. 2005), assuming that CWCs' diet derives directly from sinking algal material from the surface ocean. Otherwise, there could be an atypically large N isotope fractionation associated with the trophic-level transfer between the coral diet and its tissue (>3-3.5‰), possibly borne out of intermittent starvation periods (Doi et al., 2017), which is then communicated to the organic matrix within the coral skeleton. The gap in our understanding of how corals record the $\delta^{15}N$-PON exported form the surface ocean raises questions regarding the consistency of the offset in space and time, and whether it is apt to differ among CWC species or due to intra-specific variations in diet.

Due to the challenges of accessing deep ocean environments, the trophic ecology of cold-water corals is sparsely documented, yet is fundamental to understanding the role of CWCs in cold water reef ecosystems and to defining their utility as paleoceanographic archives of N cycling. The nature of the $\delta^{15}N$ offset between CWC skeletal material and exported PON must be explained in order to fully validate the use of CWCs as proxies to reconstruct the history of exported PON and to further understand the role of CWCs in benthic ecosystems. To this end, we studied *Balanophyllia elegans,* a scleractinian cold-water coral found along the west coast of North America that grows as individual polyps (Fadlallah, 1983). We investigated the following questions: a) Is there a large offset in $\delta^{15}N$ between coral polyp tissue and coral skeletal tissue? b) Is there an unusually large trophic-level offset between coral tissue and coral diet? c) Does *B. elegans* feed predominantly on suspended particulate organic matter (SPOM) *in situ* or d) does *B. elegans* feed predominantly on metazoan zooplankton, resulting in a two-level trophic transfer between coral tissue and N of export? To evaluate these questions, we cultured *B. elegans* corals in the laboratory under a controlled diet to document trophic isotope effects and soft tissue N turnover, we investigated the soft *vs.* skeletal tissue $\delta^{15}N$ of coral specimens collected from a field site in the Salish Sea, and we queried components of the food web at the field site. Our observations offer novel insights on the growth and trophic ecology of *B. elegans*, providing unique new data on the N metabolism of CWC and their feeding ecology. We contextualize our conclusions to inform the use of CWC archives as a paleo-proxy for marine N cycling and ocean biogeochemistry.

https://doi.org/10.5194/bg-2023-127
Preprint. Discussion started: 21 August 2023

2. Methods

2.1 Collection of live coral specimens

Individual specimens of the cold-water coral *Balanophyllia elegans* were collected during four sampling campaigns in March and June 2019, and September and November 2020 from the San Juan Channel near the University of Washington's Friday Harbor Laboratory off the coast of Washington State in the Salish Sea (48.5º N, -123.0º W; Figure 1). Specimens were collected at 10 to 20 m depth by divers who gently removed the corals from vertical rock walls using blunt-tipped diving knives. Of the live corals collected, a subset was immediately frozen at -18ºC for N isotope ratio analyses of soft tissue and organic matter bound in the coral skeleton matrix. Live specimens were shipped overnight in small bags of seawater on ice to St. Olaf College (Minnesota, USA). Corals were cleaned by gently scraping the exposed skeleton with dental tools to remove encrusting organisms and placed in incubation bottles with artificial seawater for recovery prior to feeding experiments (described below).

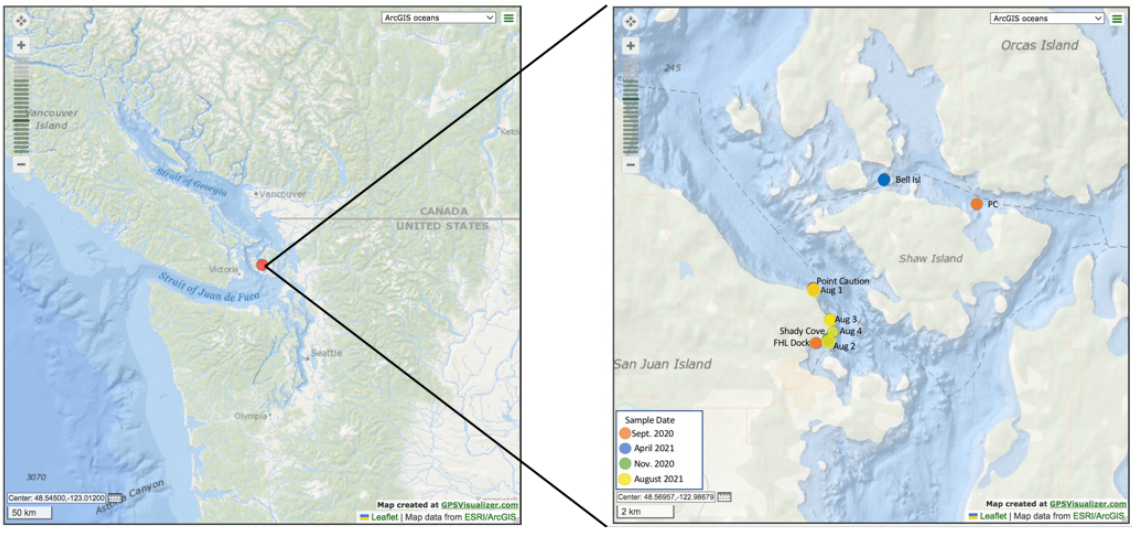

Figure 1. Map of the San Juan Islands indicating the collection site of *B. elegans* specimens and hydrographic measurements (ESRI, 2021).

2.2 Live coral maintenance

Live *B. elegans* corals were maintained in artificial seawater medium prepared from nitrate-free Instant Ocean® Sea Salt. Salts were dissolved in deionized water to a salinity of 28.0 ± 0.25 – akin to the conditions at the collection site (Murray et al., 2015) – and sparged with air to achieve atmospheric equilibrium. The pH of the seawater was measured with a YSI brand 4130 pH probe and adjusted using dilute (0.1 N) hydrochloric acid or sodium hydroxide to 8.14 ± 0.05, slightly higher than *in-situ* conditions to promote skeletal growth. Batch

https://doi.org/10.5194/bg-2023-127
Preprint. Discussion started: 21 August 2023

seawater was then allotted to 2 L airtight polypropylene bottles to incubate single coral polyps. Bottles were pre-cleaned with fragrance-free soap and multiple rinses of deionized water. The salinity, pH, and temperature in the incubation bottles were monitored using YSI brand probes (4310(W) conductivity cell and pH probe, respectively) as well as dissolved oxygen concentrations using an optical sensor (FDO 4410; Figure S1); a Multilab 4010-3w was used as the digital meter for the sensors. The bottles containing individual corals were randomly distributed among three recirculating water baths maintained at a constant temperature of 12.5 ± 0.2 ºC, akin to the conditions at the collection site (Murray et al., 2015). Small but quasi-systematic differences of ± 0.3˚C were observed among the three recirculating tanks (Figure S2). Corals were sustained on a diet of *Artemia salina* nauplii (described below), fed twice a week to ensure maximum growth (Crook et al., 2013). Seawater in the incubation bottles was replaced twice a week after the corals were fed, based on observations indicating that seawater pH in the bottles decreased slightly but significantly by ~0.03 pH units over three days due to coral respiration (statistical analysis was performed with RStudio; Welch two sample t-test; $t(515.07)= 12.8$; p-value < 0.01; Figure S3). Dissolved oxygen concentrations remained near atmospheric equilibrium at concentration of 7.5 ± 0.3 mg L^{-1} (Figure S1). Nitrate concentrations in the bottles were also monitored from samples taken during each water change, in the freshly prepared seawater and in spent seawater, revealing low variability in NO_3^- concentration of 0.7 ± 0.3 µmol L^{-1} (Figure S4). Nitrate concentrations in the incubations were notably lower than ambient levels at the collection site, where concentration were ~25 µmol L^{-1}, ensuring that the coral's only source of nitrogen was the *Artemia* diet (Murray et al., 2015).

2.3 Coral culture experiments

2.3.1 Evaluation of the trophic isotope effect and turnover time

The corals were acclimated to precise incubation conditions for approximately 20 hours before initiating feeding experiments. To assess the $\delta^{15}N$ of coral soft tissue compared to that of its food source, four experimental groups of individual *B. elegans* corals were fed respective diets of *Artemia salina* nauplii with different $\delta^{15}N$ values, twice per week for 530 days (Spero et al., 1993). Unhatched *Artemia salina* sourced from specific geographic locations have widely different $\delta^{15}N$ values, owing to the different N isotope dynamics of the environments from which they were collected, which makes these organisms useful for trophic studies (Spero et al. 1993). We refer to respective experimental groups by a color name (green, yellow, orange and pink). Eighteen coral specimens assigned to the green group were fed *Artemia* nauplii hatched from cysts from the Great Salt Lake (Reference Code: GSL) with a $\delta^{15}N$ of 17.0 ± 0.3 ‰. The yellow group consisted of twelve corals that were fed hatched nauplii from Lake Ulzhay in Russia (Reference Code: 1816) with a $\delta^{15}N$ of 13.8 ± 0.4 ‰. Twelve

https://doi.org/10.5194/bg-2023-127
Preprint. Discussion started: 21 August 2023

corals were in the orange group which was fed hatched nauplii from Vinh Chau in Vietnam (Reference Code: 1805) with a $\delta^{15}N$ of 9.9 ± 0.3‰. The pink group consisted of twelve corals that were fed hatched nauplii from Tibet (Reference Code: 1808) with $\delta^{15}N$ of 6.3 ± 0.2‰. The GSL *Artemia* was procured from Aquatic Foods California Blackworm Co. (Great Salt Lake), whereas all other *Artemia* were obtained from the Artemia Reference Center (Ghent, Belgium). The $\delta^{15}N$ of the diet for each treatment was calculated as the mean value measured from each group of unhatched cysts and hatched nauplii (Table S2 and S3).

Fresh batches of nauplii were hatched from *Artemia* cysts at approximately monthly intervals, stored frozen at -18ºC, and thawed immediately before feeding to the corals. Due to low hatch rates of the *Artemia* group 1808, corals in that treatment group were fed nauplii harvested from decapsulated *Artemia* cysts from day 151 (November 19, 2019) to 245 (February 22, 2020). The $\delta^{15}N$ of the hatched nauplii ranged from 6.3 ± 0.2 to 17.0 ± 0.3 ‰ (measured by EA-IRMS; Table S3). The $\delta^{15}N$ of the nauplii did not change significantly over prolonged storage of several months in the freezer (ANOVA test; F(1) = 0.07, p-value = 0.80; Figure S5). *Artemia* nauplii had a statistically indistinguishable molar C:N ratios among regional groups, averaging 6.0 ± 0.6 (ANOVA test; F(3) = 0.31; p-value = 0.82, Table S3).

Corals were fed their respective nauplii diets by transferring coral individuals from their incubation bottle to a small dish filled with artificial seawater. Each coral was fed 20 µL of thawed nauplii suspension by pipetting the food directly into their oral cavity, making it possible to visually ensure complete consumption and thus minimize variability in feeding rates. Each coral was returned to its bottle with a fresh allotment of seawater when its mouth had remained closed for several minutes, signifying that it was finished eating (Figure 2).

Individual corals were sacrificed at discrete intervals throughout the experiment to monitor N turnover. Corals were always sacrificed three days after feeding to ensure that no food remained in the oral cavity. The corals were removed from their bottles and rinsed with artificial seawater. The coral tissue was then separated from the skeleton using a fine stream of compressed air. The tissue and skeleton were frozen at -18ºC and stored separately until processed for isotope ratio analyses.

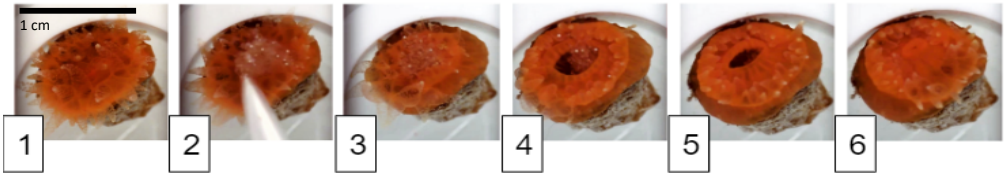

Figure 2. Photo illustration of a coral feeding sequence. Photo 1 shows coral before food is given. Photo 2 shows food being pipetted onto coral mouth. Photos 3 through 6 show the coral feeding as the mouth opens to engulf food and closes when finished, about 15 minutes in total. Corals are ~1 cm in diameter.

https://doi.org/10.5194/bg-2023-127
Preprint. Discussion started: 21 August 2023

2.3.2 *Evaluation of the effects of starvation conditions*

An additional 522-day feeding experiment was performed to assess the influence of starvation on the $\delta^{15}N$ of the coral soft tissue. Live corals collected during a sampling campaign at the end of November 2020 and shipped live to St. Olaf College were randomly assigned to two treatment groups, referred to as "long" and "short". Corals in the "long" treatment were fed every two weeks, whereas those in the "short" treatment were fed twice a week. Both groups were fed *Artemia* nauplii with a $\delta^{15}N$ of 9.9 ± 0.3 ‰, approximately 3 ‰ lower than the coral tissue of average *B. elegans* collected from Friday Harbor, and thus presumably closest in $\delta^{15}N$ to what the corals is eating in the wild. Coral incubations and feedings were conducted as described above. Individuals were sacrificed over the course of the 522-day experiment, and tissue samples were frozen at -18ºC until isotope analysis.

2.4 Coral preparation for isotope ratio analyses

Frozen coral tissue samples (and hatched nauplii) were freeze-dried using a Labconco FreeZone 4.5 and then powdered using a mortar and pestle. The samples were sent to the University of Connecticut, Avery Point (Groton, CT, USA) for isotope ratio analyses.

Coral skeletons from specimens collected at Friday Harbor were separated from the coral soft tissue and were rinsed and individually and ultrasonicated two times in Milli-Q™ (MQ) water for 20 minutes each in order to remove any residual seawater. Samples were then individually ultrasonicated in a 1% sodium hypochlorite (bleach) solution for at least two 20-minute intervals with fresh bleach for each new ultrasonication interval until no tissue remained on the skeleton, as assessed visually under a dissection microscope. Individual skeletons were then rinsed and ultrasonicated for 20 minutes in MQ another three times (each time with a new batch of MQ water) in order to remove any bleach residue. Skeleton samples were sent to Pomona College (California, USA) for further processing.

Organic material in the skeleton matrix was isolated and oxidized to nitrate following the protocol of Wang et al., (2014). Briefly, bulk samples weighing 50-100 mg were ground into coarse powder, and a fraction between 63 and 200 μm was collected by sieving through two metal sieves. The sieved powder was rinsed sequentially with of sodium polyphosphate-sodium bicarbonate buffered dithionite-citrate reagent, then treated with 13.5% sodium hypochlorite overnight on a shaker. Skeletal material was dissolved in 4 N ultrapure hydrochloric acid, then oxidized to nitrate by autoclaving in basic potassium persulfate solution. Standards of glutamine reference material USGS-40 and USGS-41 (respective $\delta^{15}N$ of 4.52 ‰ vs. air and 47.57 ‰ vs. air) were oxidized in tandem

https://doi.org/10.5194/bg-2023-127
Preprint. Discussion started: 21 August 2023

and used to correct for processing blanks. The resulting nitrate samples were sent to the University of Connecticut for nitrate isotope ratio analysis. The long-term averaged reagent blank was 0.4-0.6 µmol L^{-1}. An internal standard of ground material of the cold-water colonial scleractinian coral *Lophelia pertusa* had a long-term $\delta^{15}N$ value 8.8 ± 1.2 ‰ (n=106)

2.5 Hydrographic data

To infer the natural food source of the *B. elegans*, we collected samples for analysis of the $\delta^{15}N$ of particulate and dissolved N pools in relation to ambient hydrographic variables (temperature and salinity) near Friday Harbor, WA. Seasonal sampling campaigns were conducted in September and November 2020 and in April, June, and August 2021 (Table S1). In all but the August 2021 campaign, particulate and dissolved N samples were collected by divers at undefined depths between the surface and the depth of coral collection. Samples were stored frozen in 30 mL HDPE bottles. Surface net tows were performed with a mesh size of 120 µm; materials were stored and shipped frozen and thawed at a later time to be filtered onto pre-combusted GF/F filters (0.7µm nominal pore size) that were stored frozen pending isotope analysis. No hydrographic variables were recorded during the campaigns except in August 2021.

During the August 2021 campaign, depth profiles of temperature and salinity from the surface to 35 m were characterized with a CastAway®-CTD (conductivity temperature depth) profiler. Water samples were collected at 5 m intervals between 5 and 30 m using a Van Dorn water sampler. Water was filtered onto pre-combusted glass fiber filters (GF/F; 0.7µm nominal pore size) into pre-cleaned 30 mL HDPE bottles and stored frozen pending analyses of nitrate concentrations and nitrate isotope ratios. The corresponding filters were stored frozen for isotope ratio analysis of suspended particulate organic material (SPOM). Surface (5 m) and deeper (25 m to the surface) net tows were conducted using plankton nets with respective mesh sizes of 150 µm and 80 µm. Net tow material was filtered directly onto a pre-combusted GF/F filters and frozen pending analysis. A portion of the net tow material from the August 2021 campaign was sieved to separate size classes of 80-100 µm, 100-250 µm, ≥ 250µm, 250-500 µm, and ≥ 500 µm. Material from the respective size classes was filtered onto pre-combusted GF/F filters and frozen until isotope analysis.

2.6 Nitrate concentrations and isotope ratio analyses

Nitrate concentrations of oxidized coral skeletons and in aqueous samples were measured by reduction to nitric oxide in hot vanadium III solution followed by chemiluminescence detection of nitric oxide (Braman and Hendrix, 1989) on a Teledyne chemiluminescence NOx analyzer Model T200 (Thousand Oaks, CA).

https://doi.org/10.5194/bg-2023-127
Preprint. Discussion started: 21 August 2023

The $\delta^{15}N$ and $\delta^{13}C$ of lyophilized coral tissue samples were analyzed at the University of Connecticut on a Costech Elemental Analyzer–Isotope Ratio Mass Spectrometer (Delta V). Approximately 0.75 mg of lyophilized sample (35 µg N) was allotted into tin cups and analyzed in tandem with recognized glutamine reference materials USGS-40 and USGS-41 with respective $\delta^{15}N$ (*vs*. air) of 4.52 ‰ and 47.57 ‰ and $\delta^{13}C$ of -26.39 ‰ and 37.63 ‰ (*vs.* PDB). Replicate analyses of ($n \geq 2$) reference materials yielded an analytical precision of (±1 SD) of 0.

Nitrate N (and O) isotope ratios of aqueous seawater samples and skeleton matrix samples were analyzed at University of Connecticut using the denitrifier method (Casciotti et al., 2002; McIlvin and Casciotti, 2011; Sigman et al., 2001). The denitifier method uses denitrifying bacteria (*Pseudomonas chlororaphis* f. sp. *aureofaciens*, ATCC 13985) that lack the terminal nitrous oxide (N_2O) reductase to quantitatively convert nitrate to nitrous oxide which is measured by gas-chromatography-isotope ratio mass spectrometry. Cells were cultured in Tryptic Soy Broth (Difco; Hunt Valley, MD, USA) amended with 10 mM nitrate in stoppered glass bottles. Cells in stationary phase were harvested by centrifugation and resuspended in nitrate-free medium and dispensed as 3 mL aliquots into 10 mL glass vials, which were then sparged with dinitrogen (N_2) gas for approximately 6 hours to remove N_2O. Nitrate sample solutions (20 nmoles for seawater samples and 7 nmoles for skeleton matrix samples) were injected into the sparged vials and incubated overnight to allow for complete conversion of nitrate to N_2O gas.

The product N_2O was extracted, concentrated and purified using a custom-modified Thermo Gas Bench II equipped with a GC Pal autosampler and dual cold traps and analyzed on a Thermo Delta V Advantage continuous flow isotope ratio mass spectrometer (Casciotti et al., 2002; McIlvin and Casciotti, 2011). Individual analyses were referenced to injections of N_2O from a pure gas cylinder and standardized through comparison potassium nitrate reference materials International Atomic Energy Agency nitrate (IAEA-N3) and the isotopic nitrate reference material United States Geological Survey 34 (USGS-34), with respective $\delta^{15}N$ *vs.* air of 4.7 ‰ and -1.8 ‰ vs. air (International Atomic Energy Agency, 1995), and respective $\delta^{18}O$ of 25.61 ‰ and -27.9 ‰ vs. Vienna Standard Mean Ocean Water (VSMOW; Gonfiantini, 1995; Böhlke et al., 2003). To account for bacterial blanks and source linearity, nitrate concentrations of the standard material – diluted in N-free seawater for aqueous seawater samples and air-equilibrated milli-Q water for skeleton matrix samples – were matched to those of samples within batch analyses, and additional bacterial blanks were also measured (Weigand et al., 2016; Zhou et al., 2022). Replicate measurements ($n \geq 2$) of all samples yielded an average analytical precision (±1 SD) of 0.3‰ for both $\delta^{15}N$ and $\delta^{18}O$.

https://doi.org/10.5194/bg-2023-127
Preprint. Discussion started: 21 August 2023

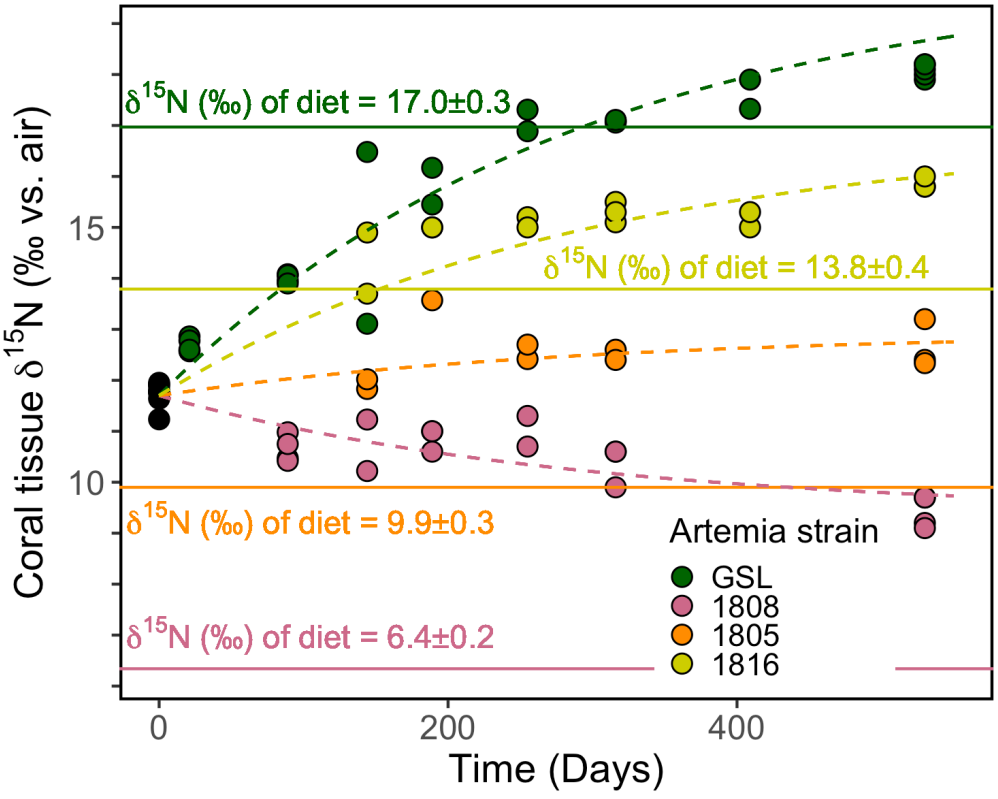

Figure 3. Evolution of the coral soft tissue $\delta^{15}N$ in response to diet $\delta^{15}N$. Colors correspond to the respective *Artemia* strains. Dashed lines are the least squares regression fits to the data using Equation 1. Solid lines mark the diet $\delta^{15}N \pm \sigma$. The mean analytical error on tissue $\delta^{15}N$ analyses was ± 0.2 ‰.

3. Results

3.1 Trophic isotope effect

At the onset of the culture experiment, the soft tissue among all experimental corals had a $\delta^{15}N$ of 11.7 ± 0.5 ‰. Over the course of the experiment, the $\delta^{15}N$ of the tissue increased or decreased in respective treatments depending on to the $\delta^{15}N$ of their *Artemia* diet (Figure 3); the tissue $\delta^{15}N$ increased in corals fed diets with $\delta^{15}N$ values of 17.0, 13.8, and 9.9 ‰, whereas the tissue $\delta^{15}N$ decreased for the diet of 6.4 ‰. The $\delta^{15}N$ of soft tissue in all groups trended towards an asymptotic offset relative to the diet $\delta^{15}N$. At day 530, at the end of the experiment, the coral tissue of the treatment groups reached $\delta^{15}N$ values of 9.4 ± 0.3‰, 12.6 ± 0.5‰, 15.9 ± 0.1 ‰, and 18.1 ± 0.1 ‰ for groups fed the lowest to highest *Artemia* $\delta^{15}N$ values, respectively. The difference

https://doi.org/10.5194/bg-2023-127
Preprint. Discussion started: 21 August 2023

between coral soft tissue and diet $\delta^{15}N$ ranged from a minimum of 1.0 ± 0.1‰ to a maximum of 3.0 ± 0.3‰ across the different experimental groups (Figure 3). Expecting the difference between coral tissue and prey $\delta^{15}N$ among experimental groups to ultimately converge, corals had evidently not reached isotopic equilibrium relative to prey by the end of the culture experiment. In order to determine the trophic $\delta^{15}N$ offset between tissue and prey and to estimate the turnover time of the coral tissue with respect to nitrogen, we fit the data to a least-squares regression corresponding to an isotope mixing model in which describes the time-dependent evolution of tissue $\delta^{15}N$ in relation to that of the diet (Eq. 1, after Cerling et al. 2007; Ayliffe et al. 2004)),

$$\delta^{15}N(t) = [\delta^{15}N_{t=0} - \delta^{15}N_{diet} + \epsilon] \cdot e^{-\lambda t} + \delta^{15}N_{diet} + \epsilon. \quad \text{Equation 1}$$

The term $\delta^{15}N_{t=0}$ is the value of the coral tissue at the onset of the experiment, $\delta^{15}N_{diet}$ is that of the corals' *Artemia* diet, t is the number of days since the start of the experiment, ϵ is the difference between the $\delta^{15}N$ of the diet and tissue at equilibrium, and λ is the specific nitrogen incorporation rate (d^{-1}), the inverse of which is the turnover time for N. Values of ϵ and λ were estimated by generating 4 simultaneous equations using the $\delta^{15}N$ of soft tissue and diet for the 4 treatments groups. The model fit yielded a trophic offset, ϵ, of 3.0 ‰ with a standard error of 0.1 ‰ between coral tissue and diet. The isotopic turnover time of N was 291 ± 15 days (λ ± standard error).

3.2 Starvation

At the onset of the starvation trial, the coral tissue had an average $\delta^{15}N$ of 11.5 ± 0.1 ‰. At the end of the 522-day experiment, the starved group (N=15 coral individuals) had an average $\delta^{15}N$ of 12.4 ± 0.4 ‰ and the frequently fed group (N=15) with a $\delta^{15}N$ of 12.7 ± 0.1 ‰. The starved group was +2.5 ± 0.4 ‰ compared to its diet, statistically indistinguishable from that of the frequently fed group of +2.8 ± 0.1 ‰ higher than the diet (p-value = 0.059, pairwise t-test; Figure 4).

https://doi.org/10.5194/bg-2023-127
Preprint. Discussion started: 21 August 2023

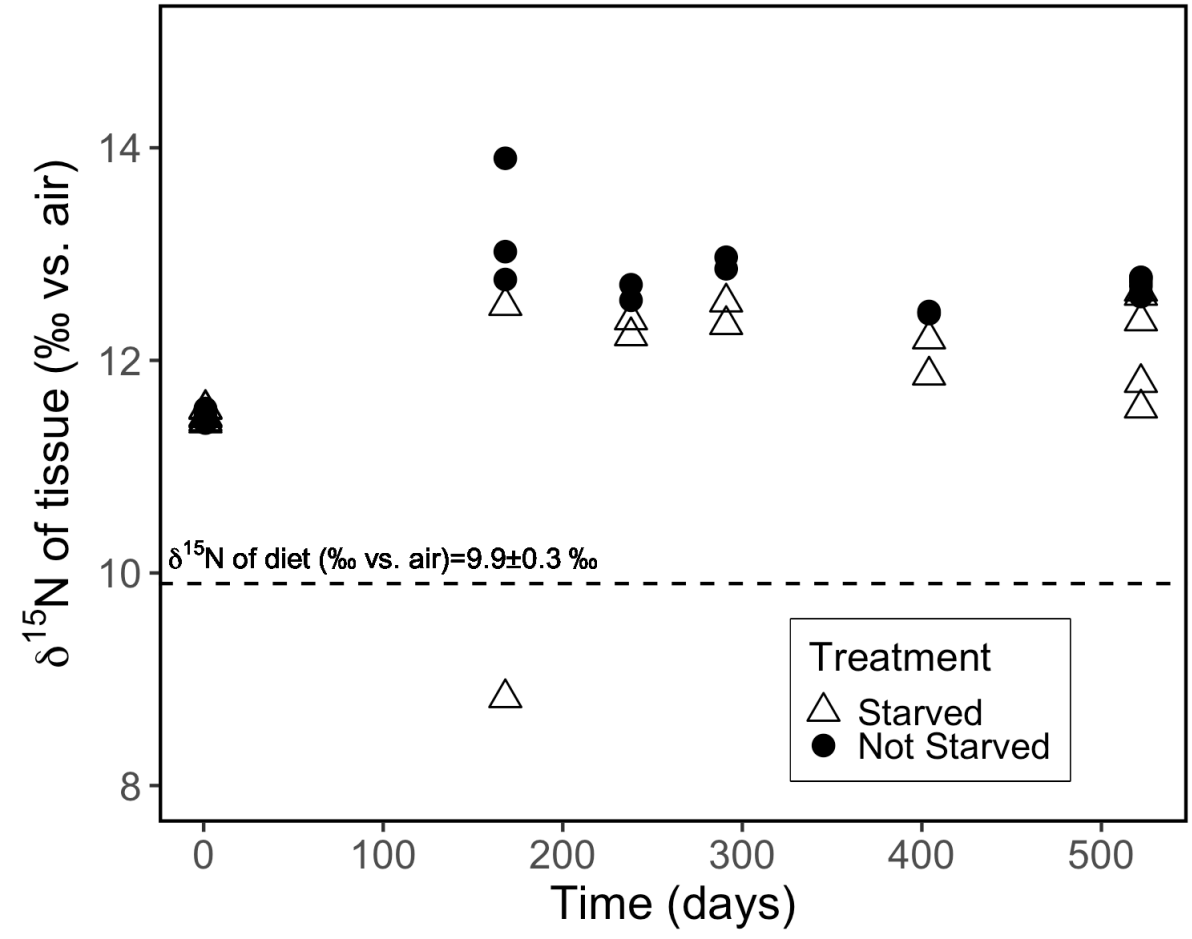

Figure 4. Evolution of the $\delta^{15}N$ of individual coral polyps fed *Artemia* nauplii ($\delta^{15}N$ 9.9 ‰) twice weekly (not starved) *vs.* every two weeks (starved). The analytical error associated with individual tissue $\delta^{15}N$ measurements was ± 0.2 ‰.

3.3 $\delta^{15}N$ comparison of field specimen polyp tissue and skeleton

The $\delta^{15}N$ of the soft tissue from individual *B. elegans* specimens collected live near Friday Harbor ranged between 11.2 to 13.1 ‰, averaging 12.0 ± 0.6 ‰ (Figure 5a). The soft tissue $\delta^{15}N$ differed among coral groups collected during different sampling campaigns, with higher values in spring (March 2019 and April 2021) compared to summer and fall (June 2019, September and November 2020; ANOVA $F(4) = 40.39$; p-value ≤ 0.01, post-hoc pairwise t-test; p-value < 0.05.). The average $\delta^{15}N$ of corresponding skeletal tissue was 13.5 ± 0.7 ‰

https://doi.org/10.5194/bg-2023-127
Preprint. Discussion started: 21 August 2023

and did not differ discernibly among sampling campaigns (ANOVA F(2) = 0.916; p-value = 0.431). The average difference between skeleton and soft tissue $\delta^{15}N$ ($\Delta\delta^{15}N$) among coral individuals for which both soft tissue and skeleton were measured was 1.2 ± 0.6 ‰ (Figure 5b).

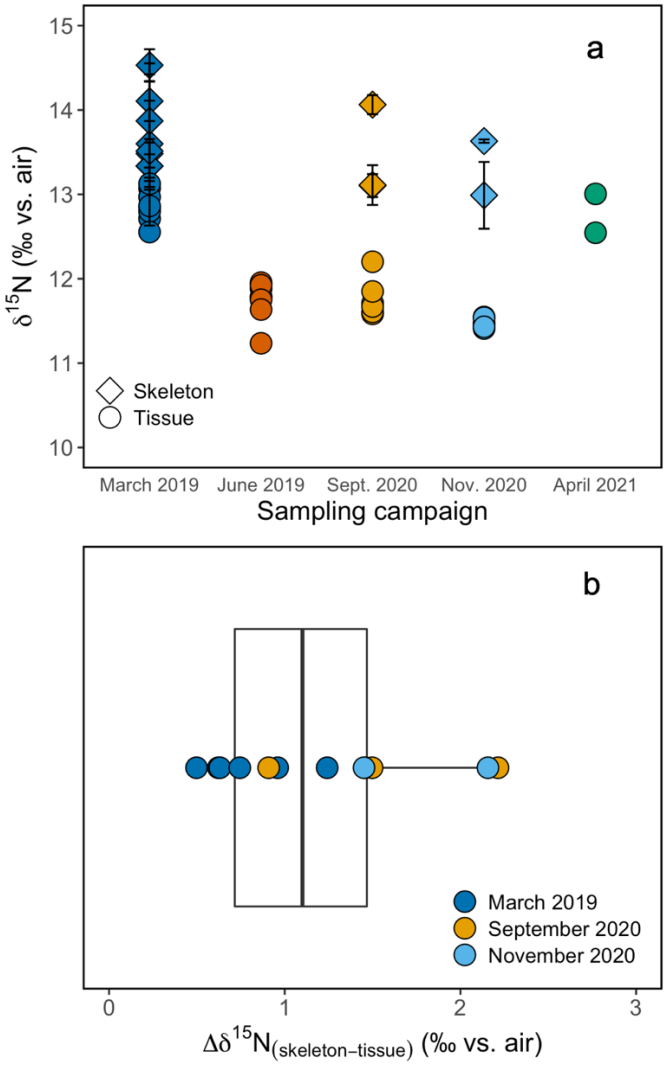

Figure 5. (a) Tissue and skeleton $\delta^{15}N$ measurements from *B. elegans* individuals collected during different sampling campaigns. Errors on skeleton $\delta^{15}N$ are given in the text. Errors on tissue data are based on measurements of replicate samples. (b) Boxplot of the difference between tissue and skeleton of individual *B. elegans* corals. The boxplot shows the mean, first and third quartile, maxima, and minima. Individual data points are overlaid on the plot. Colors correspond to respective sampling campaigns.

https://doi.org/10.5194/bg-2023-127
Preprint. Discussion started: 21 August 2023

345

346 3.4 Regional hydrography and N isotope ratios of nitrate and plankton material

347 Hydrographic profiles recorded at stations near Friday Harbor in August 2021 showed characteristic density
348 structures that were sensitive to tidal phase (Figure 6a,b; Banas et al. 1999). Profiles collected during flood tide
349 were relatively well-mixed (salinity 30, temperature 11.8˚C), with fresher and warmer water restricted to the near
350 surface (≤ 5 m), whereas ebb-tide profiles showed a progressive decrease in salinity from 30 to 27 and a
351 corresponding increase in temperature from 11.8˚C at 35 m to 14.5˚C at the surface.

352 Nitrate concentrations were nearly uniform with depth during flood tide (~20 µmol L^{-1}), decreasing slightly at
353 5 m, whereas during ebb tide nitrate concentrations decreased progressively from 20 to 10 µmol L^{-1} between 30
354 and 10 m (Figure 6c). Nitrate concentrations in samples collected during the other sampling campaigns ranged
355 from 12 to 32 µmol L^{-1}, and appeared generally higher at stations visited during the September and November
356 2020 campaigns compared to those in April and August 2021 (Figure S6).

357 Depth profiles collected in August 2021 revealed uniform nitrate $\delta^{15}N$ values at 30 m of ~7 ‰ among
358 profiles. In well-mixed profiles, nitrate $\delta^{15}N$ increased slightly to 7.5 ‰ above 10 m. In stratified profile, nitrate
359 $\delta^{15}N$ increased progressively to 8.2 ‰ at 10 m (Figure 6d). Among all sampling campaigns, the $\delta^{15}N$ of nitrate
360 ranged from 6.1 ‰ to 8.2 ‰, with median values of 6.8 ± 0.4 ‰ (Figure 7a). The relationship between nitrate
361 $\delta^{15}N$ and nitrate concentration in August 2021 was fit to a closed-system Rayleigh distillation model (Mariotti et
362 al. 1981), suggesting a nitrate assimilation isotope effect of 1.5 ± 0.1 ‰ (Figure 8).

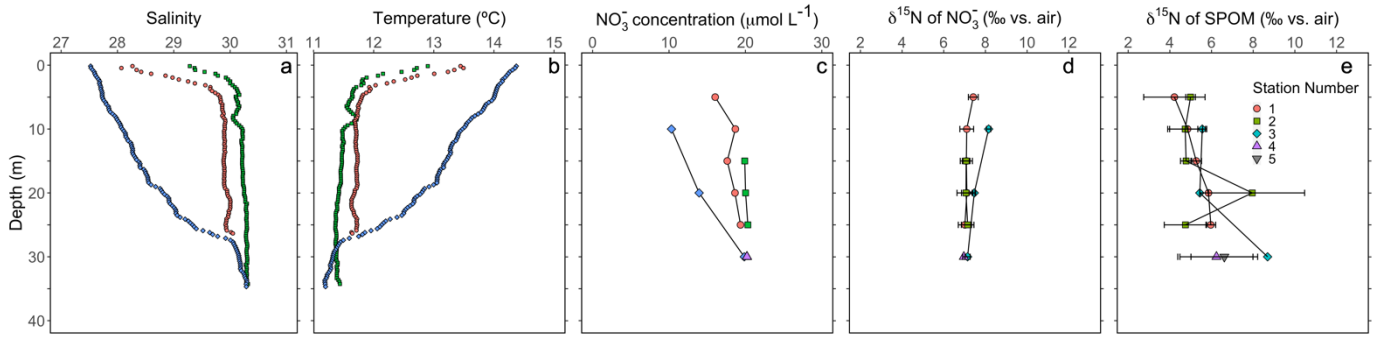

363

364 Figure 6. Depth profiles during the August 2021 sampling campaign of (a) salinity, (b) temperature, (c)
365 nitrate concentration, (d) the $\delta^{15}N$ of nitrate for analytical replicates and (e) the $\delta^{15}N$ of SPOM of replicate
366 samples (n ≥ 2). Green and red symbols correspond to flood tide, blue symbols correspond to ebb tide.

367

https://doi.org/10.5194/bg-2023-127
Preprint. Discussion started: 21 August 2023

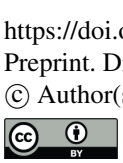

368 The $\delta^{15}N$ of SPOM collected at depths above 35 m near Friday Harbor during the different sampling
369 campaigns ranged from 1.6 to 11.7 ‰, averaging 5.7 ± 1.7‰ (Figure 7b). Values were lowest for the four
370 samples collected in spring (4.4 ± 0.4 ‰), and highest for the four samples collected in autumn (6.2 ± 2.6 ‰),
371 although these trends may be an artifact of the low data density in spring (n = 4) and autumn (n = 5) relative to
372 August 2021 (n = 29), at which time the observed range of $\delta^{15}N$ subsumed that in the other two campaigns.
373 Values did not differ coherently with depth in August 2021, although any potential depth structure was obscured
374 by the large variability among sample replicates (Figure 6e).

375 The $\delta^{15}N$ of material collected in net tows (120 µm mesh size) during sampling campaigns in September
376 2020, and June 2021 ranged between 7.9 to 8.8 ‰ (Figure 7c). Material collected in net tows of 80 µm and 150
377 µm mesh size in August 2021 and separated by size class post-collection revealed a coherent $\delta^{15}N$ increase with
378 size class (Figure 7c; Figure 9). The ≥ 80 µm size class had a mean $\delta^{15}N$ of 6.0 ± 0.3 ‰ whereas that ≥ 500 µm
379 had an average $\delta^{15}N$ of 8.0 ± 0.8 ‰, which was significantly greater than the $\delta^{15}N$ of the other size classes
380 (ANOVA, p-value <0.05).

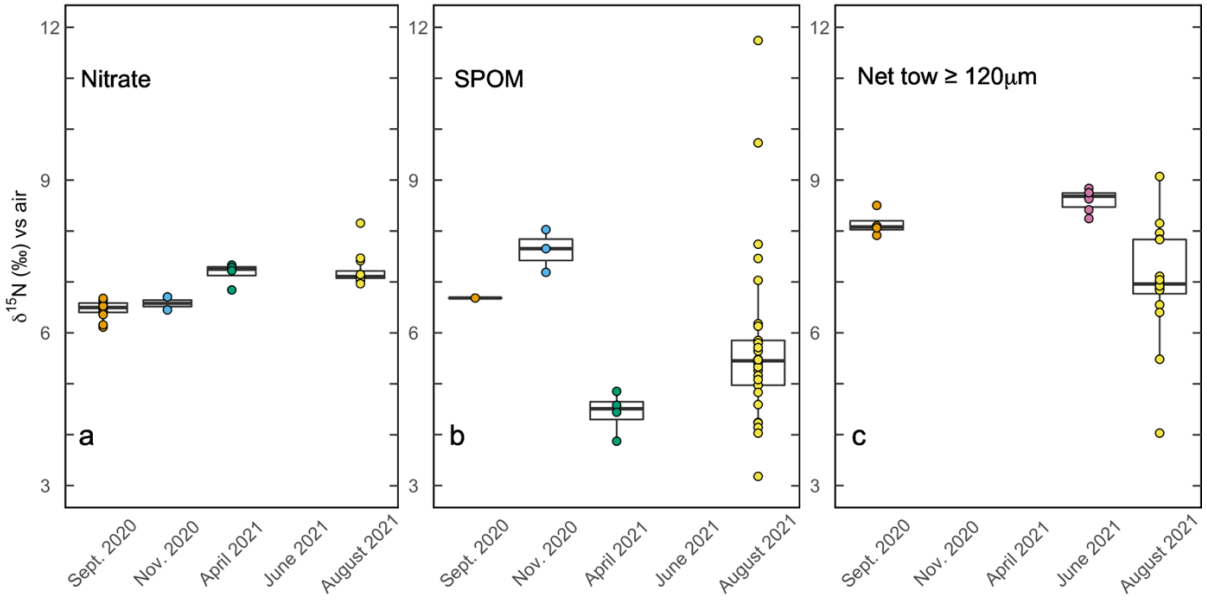

381

382 Figure 7. Boxplots of aqueous and particulate N pools at respective sampling times. (a) The $\delta^{15}N$ of nitrate
383 from samples above 30 m collected during respective sampling campaigns. (b) The $\delta^{15}N$ of suspended
384 particulate organic matter (SPOM) at sites near Friday Harbor during respective sampling campaigns. (c)
385 The $\delta^{15}N$ of net tows (≥ 120 µm mesh size) conducted during respective sampling campaigns.

https://doi.org/10.5194/bg-2023-127
Preprint. Discussion started: 21 August 2023

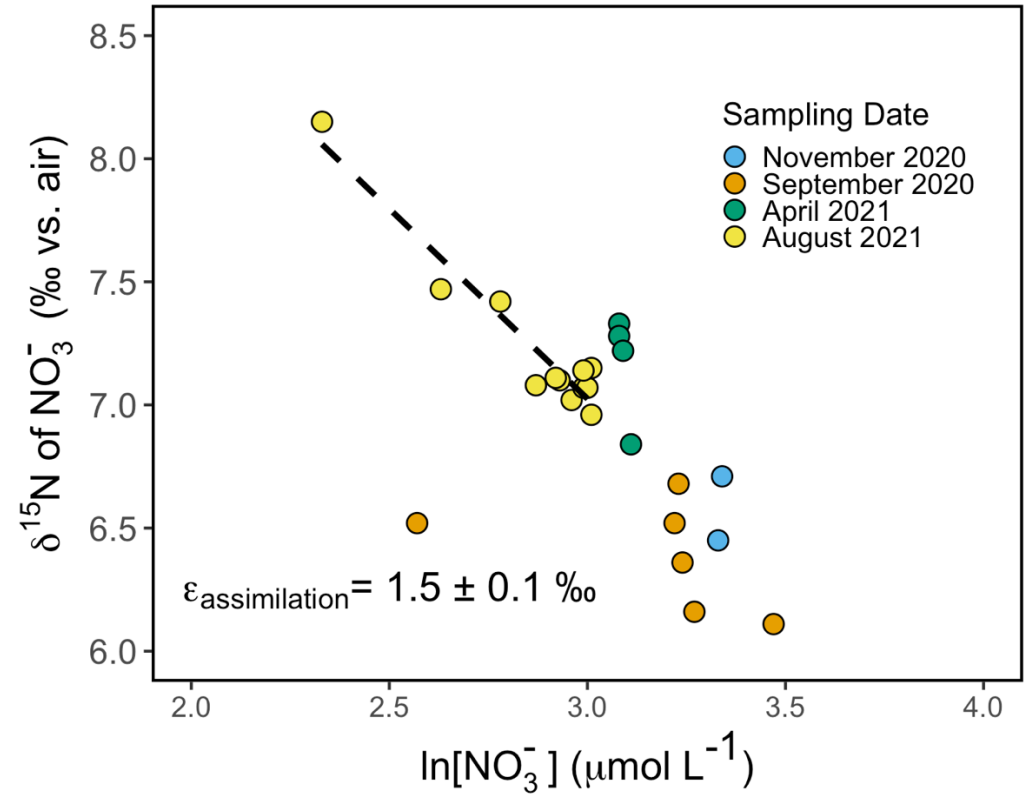

386

387 Figure 8. Rayleigh plot of nitrate $\delta^{15}N$ vs. ln of nitrate concentration for samples collected from the surface
388 to 40 m around Friday Harbor. The isotope effect of ~1.5 ± 0.1 ‰ corresponds to the slope of the best fit
389 linear regression line for the August 2021 data, $\delta^{15}N_{NO3} = 11.7 - 1.5 \ln [NO_3^-]$.

390 **4. Discussion**

391 This study of *B. elegans* provides novel constraints on the trophic ecology of scleractinian CWCs. Foremost,
392 our observations of *B. elegans* collectively suggest that the relatively large global $\delta^{15}N$ offset of 8-9 ‰ between
393 CWC skeletal tissue and the $\delta^{15}N$ of PON exported from the surface ocean is neither explained by a large
394 difference between tissue and skeleton $\delta^{15}N$, nor by an unusually large trophic isotope effect. Further, controlled
395 feeding experiments yielded direct estimates of the trophic isotope effect and the corresponding N turnover time
396 of *B. elegans* soft tissue. Examination of soft tissue $\delta^{15}N$ of wild specimens in relation to regional hydrography
397 and food web components near Friday Harbor compels us to conclude that *B. elegans* feeds predominantly
398 metazoan zooplankton prey, implicating more than one trophic transfer between PON and coral soft tissue. We
399 contextualize our findings to existing studies of CWC trophic ecology and discuss the implications of considering
400 a two-level trophic transfer for paleo-reconstructions of ocean N cycling using *B. elegans* and CWCs more
401 generally.

https://doi.org/10.5194/bg-2023-127
Preprint. Discussion started: 21 August 2023

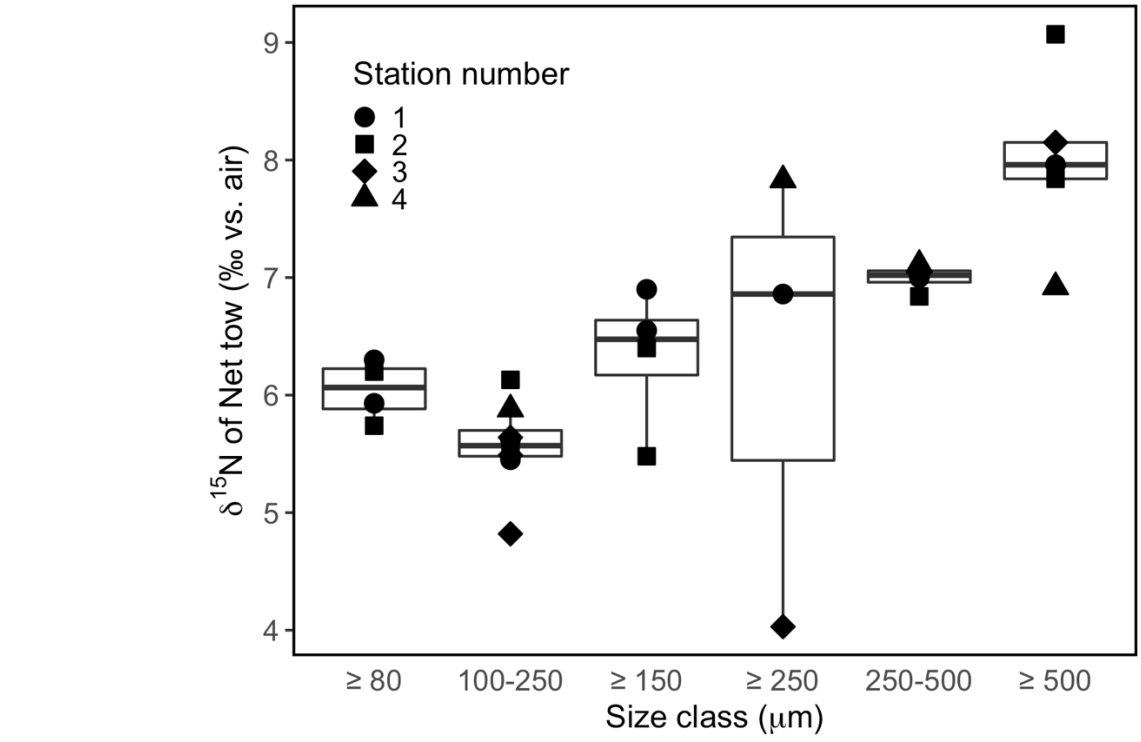

Figure 9. Boxplots of net tow material collected above 30 m in August 2021, separated by size class.

4.1 Culture experiments revealed a normal trophic isotope effect

We queried whether the large difference in $\delta^{15}N$ between PON export from the surface and coral skeleton-bound $\delta^{15}N$ (8-9 ‰) observed by Wang et al. (2014) could arise from an unusually large trophic level offset specific to CWCs. The long-term feeding experiment of *B. elegans* polyps revealed a 'normal' trophic isotopic offset between coral tissue and diet (ε of +3.0 ± 0.1 ‰ – a value that conforms to the expected range of +3.4 ± 1.1 ‰ for a single trophic level offset in $\delta^{15}N$) (Minagawa and Wada, 1984).

To support the above conclusion, we assess the assumptions inherent to the isotope mixing model (Eq. 1) used to derive ε and the corresponding nitrogen turnover from our culture data. First, the model only accounts for the turnover of a single pool of N, requiring the assumption that all N in the coral polyp tissues equilibrate at the same rate. This notion is unlikely to be wholly accurate, as turnover time varies among tissue types. However, given the relatively low resolution of our sampling over the course of the culture experiments (necessary due to constraints on numbers of total samples) we are unable to extend our model to one with multiple pools (*e.g.* as in Ayliffe et al. 2004). As soft tissues of individual coral polyps were homogenized, we suggest that the $\delta^{15}N$ values and corresponding estimate of ε thus represent the average of soft tissues with potentially different turnovers. The estimates of ε and N turnover further rely on the assumption that the nutritional quality of the respective diets among treatments was equivalent, as trophic isotope effects can be sensitive to food type. Diets low in protein can

https://doi.org/10.5194/bg-2023-127
Preprint. Discussion started: 21 August 2023

be associated with greater ε values due to internal recycling of nitrogen (Adams and Sterner, 2000; Webb et al., 1998). For instance, locusts fed a low protein diet were enriched 5.1 ‰ from their diet, compared to 2.3‰ for those fed a high protein diet (Webb et al., 1998). Conversely, a compilation of studies of various metazoan consumers raised on controlled diets suggests that high protein diets generally result in higher trophic isotope effects (~3.3 ‰) compared to more herbivorous diets (~2.2 ‰), a dynamic ascribed to higher rates of N excretion to assimilation in consumers fed high protein diets (McCutchan Jr et al., 2003). To avoid diet quality confounding our estimates, we verified that the *Artemia* prey had similar C:N ratios among treatments, ensuring a similar nutritional value.

The end-member mixing represented by Equation 1 could also be invalidated given nutritional N sources additional to the *Artemia*. Biological N_2 fixation and chemoautotrophy has been detected in association with CWC holobionts, providing some N nutrition to the corals (Middelburg et al., 2016). Our trophic isotope effect estimate was in the range expected for a single trophic transfer, arguably suggesting that N_2 fixation, if occurring, contributed modestly to the corals' nutrition; it would otherwise result in a lower value of ε given a $\delta^{15}N$ contribution of -1 to 0 ‰ (Carpenter et al. 2016). That the trophic isotope effect of the poorly fed corals did not differ from that of corals that were well-fed also argues for no sources of N additional to the *Artemia*, as starved corals would presumably increase their reliance on said source. In a related vein, N recycling between the *B. elegans* specimens and potential microbial symbionts could also dampen the trophic isotope effect relative to the *Artemia* prey and yield an over-estimate of soft tissue N turnover. The normal isotope effect evinced here argues for a modest role of N retention and recycling by microbial symbionts, in contrast to tropical symbiotic corals wherein bacterial symbionts promote substantial N retention and recycling, and consequently lower trophic isotope effects (Tanaka et al. 2018). Finally, the validity of our estimates could be sensitive to differences in feeding rates, which can influence the rate of N turnover of tissues (Martínez del Rio and Carleton, 2012; Rangel et al., 2019). Corals were fed at identical times among treatments, at a relatively high feeding rate to encourage growth (Crook et al., 2013). However, given the limited number of studies on feeding in *B. elegans*, it is difficult to compare our feeding strategy and that of this species' natural environment. Overall, we consider that the mixing model described by Equation 1 is appropriate to derive the first-order trophic isotope effect and turnover time of *B. elegans*.

Changes in metabolism due to underfeeding or prolonged fasting have the potential to increase trophic-level isotope offsets due to increased protein metabolism (Adams and Sterner, 2000). For instance, extensive amino acid recycling in overwintered adult insect larvae was cited to explain trophic isotope effects upward of 10‰ (Scrimgeour et al., 1995). A meta-analysis on the effects of starvation on consumer $\delta^{15}N$ revealed that starvation generally led to increased organism $\delta^{15}N$ by an average of 0.5 ‰, up to 4.3 ‰ (Doi et al., 2017). This dynamic was documented for the tropical symbiotic coral *Stylophora phistillata,* where heterotrophically starved corals

https://doi.org/10.5194/bg-2023-127
Preprint. Discussion started: 21 August 2023

were enriched in $\delta^{15}N$ by ~0.5 ‰ compared to frequently fed corals (Reynaud et al., 2009). The trophic isotope offset of *B. elegans* soft tissue relative to its diet, ε, was not discernibly influenced by near starvation; that of corals fed once every other week was similar to that of corals fed twice a week – in spite of visible signs of stress among the former, including relatively more sluggish feeding (Figure S7) and thinner soft tissue (data not shown). The extent to which CWCs experience significant periods of starvation *in-situ* is unclear. Deep sea coral reefs are highly productive environments with high levels of biodiversity, commensurate with a relatively high food supply (Duineveld et al., 2007; 2004; Genin et al., 1986; Roberts et al., 2006; Soetaert et al., 2016; Thiem et al., 2006; Cathalot et al. 2015). Nevertheless, periodicity and spatial heterogeneity in the food supply of CWC reefs implicate periods of lower food density (Duineveld et al. 2007; Kiriakoulakis et al. 2007). High currents, downwelling and/or vertically migrating zooplankton temporally boost the export of surface organic matter to the seabed, creating 'feast' conditions, interspersed with 'famine' periods during the non-productive season (Maier et al. 2023). Regardless, our trials suggest that starvation, if pertinent to CWC communities, does not result in greater-than-expected trophic isotope offsets, at least for *B. elegans*.

4.2 Turnover time of B. elegans

We report the first estimate of the nitrogen turnover for a non-symbiotic cold-water coral of 291 ± 15 days for *B. elegans* soft tissue. This value falls within the range of existing estimates for tropical symbiotic corals. Pulse-chase experiments with ^{15}N-nitrate conducted with fragments of the tropical symbiotic coral *Porites cylindrica* yielded a N turnover time of 370 days, and of 210 days for the tropical symbiotic coral *Acropora pulcra* (Tanaka et al. 2006; 2018). These relatively long turnover times are attributed to the recycling and retention of N within the coral-symbiont system in nutrient-deplete ecosystems. In comparison, the corresponding carbon turnover in *A. pulcra* was 18 days – compared to 210 days for N – because the system is ultimately N limited (Tanaka et al., 2006). Tanaka et al. (2018) inferred that the N turnover in *P. cylindrica* would be substantially faster than 370 days without symbionts, on the order of 56 days based on estimates of polyp-specific N uptake rates. Nevertheless, the N turnover estimated for the tropical symbiotic coral *Porites lutea* was notably shorter that *A. pulcra and P. cylindrica*, on the order of 87 days (Rangel et al., 2019), implicating different N nutritional strategies among symbiotic coral groups and/or ecosystems. The N turnover for *B. elegans* estimated here is of the same order as that for tropical symbiotic corals suggesting that cold-water species have lower growth rates and/or metabolisms compared to tropical symbiotic species, although efficient N recycling has also been documented previously in cold-water corals (Middelburg et al. 2016). The slower turnover of CWCs

https://doi.org/10.5194/bg-2023-127
Preprint. Discussion started: 21 August 2023

482 relative to their symbiotic tropical counterparts may reflect the lower temperatures of the former's habitats
483 (Miller, 1995; Thomas and Crowther 2015).

484 Constraints on N turnover also allow for calibration of the temporal resolution that is achievable with the
485 CWCs $\delta^{15}N$ proxy for marine N cycling. Corals are constantly accreting skeleton, such that coral proxies have the
486 potential to provide annual resolution (e.g. Adkins et al. 2004). In theory, a rapid N turnover in CWC could
487 record seasonal changes in regional N dynamics. A turnover time of 291 ± 15 days for N in *B. elegans* soft tissue,
488 however, signifies that the $\delta^{15}N$ of coral skeleton is unlikely to provide a faithful record of seasonal differences in
489 the $\delta^{15}N$ of the coral diet. Moreover, the turnover of the pool of N that sources the skeletal tissue may be different
490 from that of bulk tissue, and thus decoupled from the soft tissue turnover time. We suggest that CWCs can likely
491 record changes in their diet on annual or longer timescales, compatible with the ability to date CWC with
492 subdecadal resolution (Adkins et al. 2004).

493 4.3 Soft tissue vs. skeleton $\delta^{15}N$

494 A large biosynthetic $\delta^{15}N$ offset between the coral soft tissue and its skeleton could conceivably account for a
495 large $\delta^{15}N$ offset between coral skeleton-bound organic matter and N of export that is not explained by single
496 trophic level enrichment of ~3 ‰. However, the mean difference between soft tissue and skeleton-bound $\delta^{15}N$
497 among *B. elegans* specimens collected at Friday Harbor was relatively modest, on the order of +1.2 ‰, ranging
498 between +0.5 and +2.2 ‰. The observed range was dictated primarily by the variability in the $\delta^{15}N$ of the coral
499 soft tissue, as skeleton-associated $\delta^{15}N$ values were relatively invariant among specimens sampled from different
500 locations and field seasons, likely due to the fact that the amount of skeleton analyzed represented multiple years
501 worth of growth. The amount of skeleton-bound organic N is small relative to aragonite mass (2-5 µmol N per g
502 of skeleton in our samples), such that homogenization of 50-100 mg aragonite fragments may alias seasonally-
503 driven variability in skeletal $\delta^{15}N$. Soft tissue values in spring were ~1.5 ‰ higher than in summer and fall, such
504 that they appeared to record seasonal changes in diet (Figure 5a). In this regard, the asymptotic nature of the two
505 end-member isotope mixing model (Eq. 1) renders *B. elegans*'s soft tissue sensitive to seasonal changes in prey
506 $\delta^{15}N$, but not likely to reach isotopic equilibrium on seasonal timescales - given an N turnover of ~291 days, as
507 discussed above. Seasonal variations in the $\delta^{15}N$ of the food source of *B. elegans* near Friday Harbor could arise
508 from corresponding differences in the $\delta^{15}N$ of nitrate entrained to the surface driven by seasonal hydrographic
509 variability around San Juan archipelago, in the extent of surface nitrate consumption, in food web structure, or
510 from some combination of these. The data density among all but the August 2021 sampling campaign is too
511 sparse to be conclusive in this regard. Otherwise, the observed differences in soft tissue $\delta^{15}N$ may result from

https://doi.org/10.5194/bg-2023-127
Preprint. Discussion started: 21 August 2023

spatial heterogeneity in food source $\delta^{15}N$ among the different collection sites visited for respective campaigns at Friday Harbor.

As documented here for *B. elegans*, the $\delta^{15}N$ difference between coral tissue and skeleton appears to be modest among various scleractinian coral species. Specimens of the symbiotic tropical coral *Porites lutea* showed a $\delta^{15}N$ offset of +1.1 ‰ between skeleton and soft tissue, whereas the symbiotic tropical coral *Favia stelligera* revealed an insignificant offset of -0.1 ‰ (Erler et al., 2015). Similarly, no offset was observed for proteinaceous cold-water corals of the genus *Lepidisis* collected off Tasmania (Sherwood et al., 2009), whereas an offset of -1.9 ± 0.8 ‰, was reported for cold-water proteinaceous corals of the genus *Primnoa* from the Gulf of Alaska, *Isadella* from the Central California Margin, and *Kulamanamana* from the North Pacific Subtropical Gyre (McMahon et al., 2018). Conversely, a study of numerous species of both symbiotic and non-symbiotic corals reported a +4 ‰ offset between the skeletal organic matrix and soft tissue among the non-symbiotic corals specifically, but no difference among the symbiotic corals (Muscatine et al., 2005), suggesting that biosynthetic offsets may occur for certain CWC species or conditions.

4.4 Components of CWC diets

Cold water corals are considered opportunistic feeders, ingesting whatever is available in the water column (Mortensen, 2001; Freiwald, 2002; Duineveld et al. 2004; 2007; 2012; Kiriakoulakis et al. 2005; Carlier et al. 2009; Dodds et al. 2009; Van Oevelen et al. 2009). They are reported to feed on zooplankton (Kiriakoulakis et al., 2005; Naumann et al., 2011), including microzooplankton (Houlbrèque et al. 2004), on phytoplankton and phytodetritus, including the bacterial fraction of phytodetritus (Maier et al., 2020; Houlbrèque et al. 2004), dissolved organic matter (Mueller et al., 2014; Ferrier 1991, Al-Moghrabi et al. 1993; Hoegh-Guldberg & Williamson 1999; Houlbrèque et al. 2004; Grover et al. 2008), and the CWC holobiont has been observed to display biological N_2 fixation and chemoautotrophy (Middelburg et al. 2016). There is a lack of consensus, however, regarding which components of the food web dominate their diets. The soft tissue $\delta^{15}N$ of *B. elegans* specimens collected at Friday Harbor averaged 12.0 ‰, signifying that they fed on material with a $\delta^{15}N$ of approximately 9.0 ‰ – accounting for a normal trophic offset relative to their diet (3 ‰).

We first explore whether the SPOM fraction of the food web was the dominant component of *B. elegans'* diet at Friday Harbor. SPOM is operationally defined as the particulate material retained onto glass fiber filters (GF/F) from aqueous samples. At the ocean surface, including at the stations near Friday Harbor, SPOM is generally dominated by phytoplankton material. At the ocean subsurface, SPOM derives from organic material exiting the ocean surface, but is considered a distinct pool from the ballasted sinking PON collected in sediment traps. The $\delta^{15}N$ of SPOM in the ocean subsurface can be upwards of ~4-5 ‰ heavier than the corresponding sinking particles at abyssal depths due to recycling and remineralization (Altabet, 1988; Casciotti et al., 2008; Saino and Hattori, 1987). Wang et al. (2014) reasoned that because the $\delta^{15}N$ of SPOM is approximately one trophic level lower that of the N preserved in skeletons of the deep-dwelling CWC *Desmophyllum dianthus,* and because suspended particles are the most abundant form of small particles in the deep ocean, *D. dianthus* must feed predominantly on SPOM. However, SPOM collected in the upper 30 meters near Friday Harbor was ~ 6 ‰ lower than *B. elegans* soft tissue, a difference greater than expected for a single trophic level. The SPOM at Friday Harbor was evidently not the predominant food source for *B. elegans* growing in this depth interval. A

https://doi.org/10.5194/bg-2023-127
Preprint. Discussion started: 21 August 2023

more parsimonious explanation to account for the relatively high $\delta^{15}N$ of *B. elegans* soft tissue at Friday Harbor is that they derived nutrition predominantly from metazoan zooplankton. A direct positive relationship between $\delta^{15}N$ of material collected in net tows and particle size suggests that *B. elegans* consumed the largest size class of net tow material (≥ 500 µm), whose $\delta^{15}N$ was ~3.5 ‰ lower than coral soft tissue – approximating a single trophic transfer. At Friday Harbor, the net tow material had a molar C:N ratio of 4.4 ± 0.6, compared to 6.5 ± 2.2 for the SPOM (Figure S8), suggesting a higher protein content and nutritional density in the former (Adams and Sterner, 2000).

Despite evidence for zooplankton as the main dietary source for *B. elegans*, we acknowledge feeding strategies may differ among asymbiotic coral species and that CWCs may obtain nutrients from a wide range of sources when necessary. For instance, N and C isotope ratios among gorgonian soft coral species collected off the coast of Newfoundland suggest that some feed predominantly on fresh phytodetritus, while others rely on microplankton and display higher trophic levels (Sherwood et al., 2008). Additionally, some asymbiotic corals may produce mucus nets to capture suspended particles, whereby corals disperse mucus filaments with their mouth and tentacles and the particles entrapped by the mucus are then drawn back into the mouth for feeding (Lewis and Price, 1975). We observed mucus production by *B. elegans* only when polyps were out of water – a behavior ascribed to the mitigation of dessication (Brown and Bythell, 2005).

The assertion that metazoan zooplankton are the dominant dietary component of scleractinian CWCs – despite their ability to be omnivorous – is indeed supported by a number of independent studies. The single trophic level between the $\delta^{15}N$ of zooplankton prey and the soft tissue of many asymbiotic corals has generally been interpreted to indicate that zooplankton are the dominant component of their diet (Duineveld et al., 2004, Sherwood et al. 2005; 2008; 2009; Carlier et al., 2009; Hill et al., 2014; Maier et al., 2020). Additional evidence from lipid biomarkers corroborates the assertion that deep-dwelling CWC species such *Lophelia pertusa* and *Madrepora oculata* feed predominantly on metazoan zooplankton (Dodds et al., 2009; Kiriakoulakis et al., 2005; Naumann et al. 2015). Deep-dwelling CWCs (*Desmophylum pertusum, Madrepora oculata, Dendrophyllia cornigera*) also exhibit prey preference for larger zooplankton (Da Ros et al. 2022), suggesting that zooplankton prey are an essential component of their diet. Indeed, an exclusive diet of phytodetritus did not satisfy the fatty acid requirements of *Lophelia pertusa*, requiring supplementation with metazoan zooplankton to achieve maximum growth (Maier et al., 2019). Similarly, zooplankton exclusion from the diet of the solitary CWC *D. dianthus* resulted in a decrease in coral respiration (Naumann et al. 2011). More fundamentally, the shared traits of tentacles and nematocysts are evidence of a predatory life strategy, indicating that zooplankton are an important food source for corals (Lewis and Price, 1975; Sebens et al., 1996). The coral morphology of *B. elegans* and that of other cold water scleractinian corals is consistent with an adaptation for the capture of prey of a commensurate size (Fautin, 2009). Correspondingly, *D. dianthus* is considered to be a generalized zooplankton predator that can prey on medium to large copepods and euphasiids (Höfer et al., 2018). In contrast, gorgonian corals that do not capture naturally occurring zooplankton and have a correspondingly low density of nematocysts (Lasker 1981).

https://doi.org/10.5194/bg-2023-127
Preprint. Discussion started: 21 August 2023

586 Cold-water reefs are locations of high biodiversity and productivity where zooplankton prey are recurrently
587 abundant (Maier et al. 2023). Reefs occur at locales of accelerated currents that enhance the particle supply and
588 seabed productivity (Carlier et al., 2009; Maier et al., 2019). For instance, numerical simulations of circulation
589 along the Norwegian continental shelf revealed that *Lophelia pertusa* reefs correspond to locations where there is
590 a consistently high food supply entrained by Ekman transport in the benthic layer (Thiem et al., 2006). High
591 densities of zooplankton populations have been recorded in cold-water reefs between 100 and 200 m (Garcia-
592 Herrera et al., 2022), and reef zooplankton have shown preference for corals as a substrate type for hiding during
593 diel migration, implying the corals' access to zooplankton prey (Alldredge and King, 1977). The zooplankton
594 prey at abyssal depths correspondingly rely on a relatively large food supply in the benthic boundary layer, and
595 show grazing rates comparable to those in the nearshore (Wishner and Meise-Munns, 1984). Notably, the amino
596 acid-specific $\delta^{15}N$ and $\delta^{15}C$ analysis of abyssal zooplankton indicates that communities are sustained by sinking
597 phytodetritus, not by suspended particles (Carlier et al., 2009; Hannides et al. 2013), again supporting a two-level
598 trophic transfer for CWCs.

599 4.5 Does coral-bound $\delta^{15}N$ reflect surface ocean processes at Friday Harbor?

600 The effectiveness of coral skeleton-bound $\delta^{15}N$ as an archive to reconstruct past ocean N cycling depends on
601 its faithfulness to the $\delta^{15}N$ of the surface PON export. In turn, the $\delta^{15}N$ imparted to the phytoplankton component
602 of surface particles, from which PON export derives, is highly dependent on surface ocean dynamics that
603 influence the degree of nitrate consumption and associated isotope fractionation. Given complete assimilation of
604 inorganic N pools, the $\delta^{15}N$ of phytoplankton material - the dominant component of SPOM at the surface ocean -
605 converges on the $\delta^{15}N$ of the N sources, new nitrate and recycled N sources (Treibergs et al., 2014; Fawcett et al.
606 2011). At steady state, the $\delta^{15}N$ of the sinking PON flux reflects the isotope signature of the nitrate upwelled to
607 the surface (Altabet, 1988). Alternatively, given partial nitrate consumption in the context of a finite pool
608 (Rayleigh dynamic), such as in HNLC regions and in upwelling systems, the SPOM $\delta^{15}N$ is fractionated relative
609 to the nitrate $\delta^{15}N$ as function of the assimilation isotope effect and the extent of nitrate consumption (Sigman et
610 al., 1999). The $\delta^{15}N$ of the sinking flux then reflects both the $\delta^{15}N$ of nitrate upwelled to the surface and the
611 degree of nitrate consumption (Altabet and François 1994; François et al. 1997).-In this section, we discuss
612 whether coral-bound $\delta^{15}N$ reflects the $\delta^{15}N$ of nitrate entrained to the surface.

613 Nitrate assimilation at Friday Harbor was ostensibly incomplete, potentially implicating the fractionation of
614 N isotopes between nitrate and biomass. Although low surface nitrate concentrations are generally expected at
615 coastal sites during the summer due to phytoplankton assimilation, nitrate concentrations at Friday Harbor in

https://doi.org/10.5194/bg-2023-127
Preprint. Discussion started: 21 August 2023

August of 2021were upwards of 15 µM at the surface and 20 µM at 30 m depth. Indeed, nitrate in the San Juan Channel is replete year-round, even at the surface, due to vigorous mixing within the channel (Mackas and Harrison, 1997; Murray et al., 2015). The region experiences tidal mixing, designating Juan de Fuca Strait as a well-mixed estuary with minimal vertical density gradients (Banas et al., 1999; Mackas and Harrison, 1997). Nutrients are supplied to the broader region by upwelling (Lewis, 1978; Murray et al., 2015; Mackas and Harrison, 1997). The water in the San Juan Channel comprises a mix of high nutrient deep water from the Juan de Fuca Strait and fresher surface water from the Strait of Georgia (Banas et al., 1999). Nutrient concentrations in the surface Georgia Strait vary seasonally and are depleted during the summer at the stratified, fresher surface (Del Bel Belluz et al., 2021; Mackas and Harrison, 1997). The temperature-salinity plots in August 2021 corroborate end-member mixing of more saline and colder water from the Juan de Fuca Strait with fresher and warmer surface water from the Georgia Strait (Figure S9; Banas et al., 1999). The influence of Georgia Strait surface water is recognized by the salinity minima originating from the outflow of the Fraser River (Figures S10; Mackas and Harrison, 1997).

The $\delta^{15}N$ of nitrate measured at stations near Friday Harbor corroborate the mixing of nitrate-rich deeper water with nitrate-deplete surface water from Georgia Strait. The apparent isotope effect for nitrate assimilation in August 2021 was ~1.5 ‰, markedly lower than the canonical value of 5 ‰ associated with nitrate assimilation by surface ocean phytoplankton communities (DiFiore et al., 2006; Sigman et al., 1999; Altabet and François, 1994). A low apparent isotope effect is consistent with end-member mixing of lower $\delta^{15}N$, nitrate-rich water with highly fractionated (high $\delta^{15}N$), low-nitrate water (Sigman et al., 1999). Highly fractionated (assimilated) nitrate, in turn, likely originated from Georgia Strait surface waters entrained into the Channel Islands. The linear relationship between salinity and nitrate concentration in August 2021 further corroborates physical mixing as the dominant control on nitrate concentrations and isotope ratios in San Juan Channel (Figure S10; Mackas and Harrison, 1997). Moreover, the $\delta^{15}N$ of nitrate was relatively uniform with depth, indicating effective mixing. The relatively slight decrease in nitrate $\delta^{15}N$ with depth suggests a secondary influence of local nitrate assimilation on its concentration and isotope ratios.

The corresponding $\delta^{15}N$ of SPOM at Friday Harbor covered a broad range, from 4.2 ‰ to 8.7 ‰ in August 2021. The depth distribution of SPOM did not mirror the corresponding nitrate $\delta^{15}N$ profile, as could otherwise be expected. At the stratified near-surface (5 m) at station 1, the $\delta^{15}N$ of SPOM averaged 4.2 ‰ compared to 7.4 ‰ for nitrate, suggesting that particulate material at the surface consisted primarily of the instantaneous product of nitrate assimilation (Mariotti et al., 1981). The lower $\delta^{15}N$ SPOM values could also reflect some degree of reliance on regenerated N species, whose $\delta^{15}N$ is generally lower than incident nitrate (Fawcett et al., 2011; Lourey et al., 2003; Treibergs et al., 2014). Deeper in the water column, the $\delta^{15}N$ of SPOM converged on the

https://doi.org/10.5194/bg-2023-127
Preprint. Discussion started: 21 August 2023

$\delta^{15}N$ of incident nitrate, suggesting that SPOM derived from the complete consumption of an incident nitrate pool (even though nitrate was present at these depths). Phytoplankton at these depths may thus have originated from surface water entrained from the Strait of Georgia – where nitrate was completely utilized. The above dynamics complicate validation of the offset between $\delta^{15}N$ nitrate and coral-bound $\delta^{15}N$. Nevertheless, the offset between nitrate $\delta^{15}N$ and coral skeleton $\delta^{15}N$ was on the order of ~6.5 ‰, similar to the empirical range observed for other CWC species (Wang et al. 2014), suggesting that the $\delta^{15}N$ imparted on local *B. elegans* skeletons reflects the $\delta^{15}N$ of nitrate entrained to the surface, relatively unaltered by surface nitrate fractionation from partial assimilation.

5. Conclusions and implications for paleo-reconstruction from coral $\delta^{15}N$

We conclude that the solitary scleractinian cold water coral *B. elegans* predominantly derives nutrition from metazoan zooplankton prey. While our study was limited to shallower-dwelling organisms, a review of related studies corroborates that while CWCs may be able to feed on a variety of substrates, other species of scleractinian CWCs similarly rely on zooplankton prey as a fundamental component of their diet, even at abyssal depths. SPOM may contribute to CWCs' diet, but it cannot be presumed to intrinsically account for the large offset between $\delta^{15}N$ of PON export and coral skeleton $\delta^{15}N$ documented by Wang et al. (2014). The $\delta^{15}N$ of skeletal material recovered from coral archives is thus likely to be sensitive to local food web dynamics; for a given $\delta^{15}N$ of sinking PON exiting the surface ocean, the $\delta^{15}N$ recorded by CWC may differ among individuals of the same species feeding on different zooplankton prey. In this regard, the depth at which corals reside may be an important determinant of their trophic level, due to a documented increase in degree of carnivory of zooplankton with depth (Dodds et al., 2009; Vinogradov, 1962). For instance, Hannides et al. (2013) recorded a 3.5 ‰ increase in zooplankton $\delta^{15}N$ from 150 m to 1000 m in the Subtropical North Pacific, with the steepest rate of increase from 100 – 300 m. The $\delta^{15}N$ recorded in CWC skeletons is also apt to differ among species, as respective species occupy different nutritional niches (Teece et al., 2011).

Consideration of the sensitivity of the coral-bound $\delta^{15}N$ to food web dynamics informs the questions that can be adroitly addressed with the proxy, and the relationship of CWC species represented in fossil archives to the depth structure of zooplankton prey warrants further investigation. Although we do not have direct estimates of the $\delta^{15}N$ range that can be expected from local food web variability, the scatter around the global compilation of Wang et al. (2014) for coral-bound $\delta^{15}N$ of *D. dianthus* relative to the $\delta^{15}N$ of PON suggests that this range is modest, on the order of ~1-2 ‰. Given this range, we suggest that the coral-bound $\delta^{15}N$ proxy is most useful in systems where the temporal dynamic range in $\delta^{15}N$ is relatively large, and where coral specimens comprise the same species collected at comparable depths (*e.g.*, Wang et al. 2017; Chen et al. 2023). If used in this way, the broad geographic and temporal coverage afforded by CWCs, the opportunity to measure multiple proxies from individual specimens and the imperviousness of coral-bound $\delta^{15}N$ to diagenetic alteration render it a valuable paleo-proxy for reconstructing marine N cycling.

https://doi.org/10.5194/bg-2023-127
Preprint. Discussion started: 21 August 2023

Data Availability Data presented in this paper is available at: https://www.bco-dmo.org/project/893811

Author Contribution JG, AG, and MP conceptualized the research presented in this paper. JM and AG designed and carried out culture experiments. MP and AC prepared coral samples for analysis. JM and VR analyzed samples. JM, AG, JG and KD collected water samples, SPOM, and net tows. KD collected live corals for culture experiments and field studies. JM and JG prepared the manuscript with contributions from all co-authors.

Competing Interests The authors declare that they have no conflict of interest.

Acknowledgements

We are grateful to Friday Harbor Labs for their assistance with coral collections and field sampling, especially Pema Kitaeff and Megan Dethier. We acknowledge the valued assistance of the Artemia Reference Center (specifically Gilbert Van Stappen and Christ Mahieu). Coral culture experiments would not have been sustained without the help of St. Olaf undergraduate students Rachel Raser, Joash Daniel, Quintiantian Nong, YiWynn Chan, Mansha Haque, and Miranda Lenz. We are also indebted to Dr. C. Tobias and P. Ruffino for access to and assistance with the Elemental Analyzer Isotope Ratio Mass Spectrometer. This projected was funded by an NSF RUI award to A.G. (OCE-1949984), M.G.P (OCE-1949132) and J.G. (OCE-1949119).

References

Adams, T.S., Sterner, R.W. 2000. The effect of dietary nitrogen content on trophic level ^{15}N enrichment. Limnol. Oceanogr. 45, 601–607. https://doi.org/10.4319/lo.2000.45.3.0601

Adkins, J.F., Henderson, G.M., Wang, S.-L., O'Shea, S., Mokadem, F. 2004. Growth rates of the deep-sea Scleractinia *Desmophyllum cristagalli* and *Enallopsammia rostrata*. Earth and Planetary Science Letters 227, 481-490. https://doi.org/10.1016/j.epsl.2004.08.022

Alldredge, A.L., King, J.M., 1977. Distribution, abundance, and substrate preferences of demersal reef zooplankton at Lizard Island Lagoon, Great Barrier Reef. Mar. Biol. 41, 317–333. https://doi.org/10.1007/BF00389098

Al-Moghrabi, S., Allemand, D. & Jaubert, J. 1993. Valine uptake by the scleractinian coral *Galaxea fascicularis:* characterization and effect of light and nutritional status. *J Comp Physiol B* **163**, 355–362. https://doi.org/10.1007/BF00265638

Altabet, M.A., 1988. Variations in nitrogen isotopic composition between sinking and suspended particles: implications for nitrogen cycling and particle transformation in the open ocean. Deep Sea Res. Part Oceanogr. Res. Pap. 35, 535–554. https://doi.org/10.1016/0198-0149(88)90130-6

Altabet, M.A., Deuser, W.G., Honjo, S., Stienen, C., 1991. Seasonal and depth-related changes in the source of sinking particles in the North Atlantic. Nature 354, 136–139. https://doi.org/10.1038/354136a0

Altabet, M.A., Francois, R., 1994. Sedimentary nitrogen isotopic ratio as a recorder for surface ocean nitrate utilization. Glob. Biogeochem. Cycles 8, 103–116. https://doi.org/10.1029/93GB03396

Altabet, M., Higginson, M. & Murray, D. 2002. The effect of millennial-scale changes in Arabian Sea denitrification on atmospheric CO_2. *Nature* **415**, 159–162. https://doi.org/10.1038/415159a

https://doi.org/10.5194/bg-2023-127
Preprint. Discussion started: 21 August 2023

723 Ayliffe, L.K., Cerling, T.E., Robinson, T., West, A.G., Sponheimer, M., Passey, B.H., Hammer, J., Roeder, B.,
724 Dearing, M.D., Ehleringer, J.R., 2004. Turnover of carbon isotopes in tail hair and breath CO2 of horses
725 fed an isotopically varied diet. Oecologia 139, 11–22. https://doi.org/10.1007/s00442-003-1479-x

726 Banas, N., Bricker, J., Carter, G., Gerdes, F., Martin, W., Nelson, E., Ross, T., Scansen, B., Simons, R., Wells,
727 M., 1999. Flow, Stratification, and mixing in San Juan Channel.

728 Böhlke, J.K., Mroczkowski, S.J., Coplen, T.B., 2003. Oxygen isotopes in nitrate: new reference materials for
729 18O:17O:16O measurements and observations on nitrate-water equilibration. Rapid Commun. Mass
730 Spectrom. RCM 17, 1835–1846. https://doi.org/10.1002/rcm.1123

731 Braman, R.S., Hendrix, S.A., 1989. Nanogram nitrite and nitrate determination in environmental and biological
732 materials by vanadium(III) reduction with chemiluminescence detection. Anal. Chem. 61, 2715–2718.
733 https://doi.org/10.1021/ac00199a007

734 Brandes, J.A., Devol, A.H., 2002. A global marine-fixed nitrogen isotopic budget: Implications for Holocene
735 nitrogen cycling. Glob. Biogeochem. Cycles 16, 67-1-67–14. https://doi.org/10.1029/2001GB001856

736 Brown, B. E., & Bythell, J. C. 2005. Perspectives on mucus secretion in reef corals. *Marine Ecology Progress*
737 *Series*, *296*, 291–309. http://www.jstor.org/stable/24868640Cairns, S.D., 2007. Deep-water corals: an
738 overview with special reference to diversity and distribution of deep-water scleractinian corals. Bull.
739 Mar. Sci. 81, 311–322.

740 Carlier, A., Guilloux, E.L., Olu, K., Sarrazin, J., Mastrototaro, F., Taviani, M., Clavier, J., 2009. Trophic
741 relationships in a deep Mediterranean cold-water coral bank (Santa Maria di Leuca, Ionian Sea). Mar.
742 Ecol. Prog. Ser. 397, 125–137. https://doi.org/10.3354/meps08361

743 Carpenter, E. J., Harvey, H. R., Fry, B. & Capone, D. G. 1997. Biogeochemical tracers of the marine
744 cyanobacterium Trichodesmium. Deep-Sea Res. I 44, 27–38. doi.org/10.1016/S0967-0637(96)00091-X

745 Casciotti, K.L., Sigman, D.M., Hastings, M.G., Böhlke, J.K., Hilkert, A., 2002. Measurement of the oxygen
746 isotopic composition of nitrate in seawater and freshwater using the denitrifier method. Anal. Chem. 74,
747 4905–4912. https://doi.org/10.1021/ac020113w

748 Casciotti, K.L., Trull, T.W., Glover, D.M., Davies, D., 2008. Constraints on nitrogen cycling at the subtropical
749 North Pacific Station ALOHA from isotopic measurements of nitrate and particulate nitrogen. Deep Sea
750 Res. Part II Top. Stud. Oceanogr. 55, 1661–1672. https://doi.org/10.1016/j.dsr2.2008.04.017

751 Cathalot C, Van Oevelen D, Cox TJS, Kutti T., Lavaleye M., Duineveld G., Meysman F. J. R. 2015. Cold-water
752 coral reefs and adjacent sponge grounds: hotspots of benthic respiration and organic carbon cycling in the
753 deep sea. *Front Mar Sci* 2. https://www.frontiersin.org/articles/10.3389/fmars.2015.00037.

754 Cerling, T.E., Ayliffe, L.K., Dearing, M.D., Ehleringer, J.R., Passey, B.H., Podlesak, D.W., Torregrossa, A-M.,
755 West, A.G. 2007. Determining biological tissue turnover using stable isotopes: the reaction progress
756 variable. Ecophysiology 151, 175-189. https://doi.org/10.1007/s00442-006-0571-4

757 Chen, WH., Ren, H., Chiang, J.C.H. *et al.* Increased tropical South Pacific western boundary current transport
758 over the past century. *Nat. Geosci.* **16**, 590–596 (2023). https://doi.org/10.1038/s41561-023-01212-4

759 Cheng, H., Adkins, J., Edwards, R.L., Boyle, E.A., 2000. U-Th dating of deep-sea corals. Geochim. Cosmochim.
760 Acta 64, 2401–2416. https://doi.org/10.1016/S0016-7037(99)00422-6

https://doi.org/10.5194/bg-2023-127
Preprint. Discussion started: 21 August 2023

761 Cohen, A.L., Gaetani, G.A., Lundälv, T., Corliss, B.H., George, R.Y., 2006. Compositional variability in a cold-
762 water scleractinian, *Lophelia pertusa*: New insights into "vital effects." Geochem. Geophys. Geosystems
763 7. https://doi.org/10.1029/2006GC001354

764 Corbera, G., Lo Iacono, C., Simarro, G. *et al.* 2022. Local-scale feedbacks influencing cold-water coral growth
765 and subsequent reef formation. *Sci Rep* **12**, 20389. https://doi.org/10.1038/s41598-022-24711-7

766 Crook, E.D., Cooper, H., Potts, D.C., Lambert, T., Paytan, A., 2013. Impacts of food availability and pCO2 on
767 planulation, juvenile survival, and calcification of the azooxanthellate scleractinian coral Balanophyllia
768 elegans. Biogeosciences 10, 7599–7608. https://doi.org/10.5194/bg-10-7599-2013

769 Da Ros, Z., Dell'Anno, A., Fanelli, E., Angeletti, L., Taviani, M., Danovaro, R., 2022. Food preferences of
770 Mediterranean cold-water corals in captivity. Front. Mar. Sci. 9.

771 Del Bel Belluz, J., Peña, M.A., Jackson, J.M., Nemcek, N., 2021. Phytoplankton composition and environmental
772 drivers in the Northern Strait of Georgia (Salish Sea), British Columbia, Canada. Estuaries Coasts 44,
773 1419–1439. https://doi.org/10.1007/s12237-020-00858-2

774 De Pol-Holz R, Robinson RS, Hebbeln D, Sigman DM, Ulloa O. 2009. Controls on sedimentary nitrogen
775 isotopes along the Chile margin. *Deep Res Part II Top Stud Oceanogr* 56(16).
776 doi:10.1016/j.dsr2.2008.09.014

777 DiFiore, P.J., Sigman, D.M., Trull, T.W., Lourey, M.J., Karsh, K., Cane, G., Ho, R., 2006. Nitrogen isotope
778 constraints on subantarctic biogeochemistry. J. Geophys. Res. Oceans 111.
779 https://doi.org/10.1029/2005JC003216

780 Dodds, L.A., Black, K.D., Orr, H., Roberts, J.M., 2009. Lipid biomarkers reveal geographical differences in food
781 supply to the cold-water coral *Lophelia pertusa* (Scleractinia). Mar. Ecol. Prog. Ser. 397, 113–124.
782 https://doi.org/10.3354/meps08143

783 Doi, H., Akamatsu, F., González, A.L., 2017. Starvation effects on nitrogen and carbon stable isotopes of
784 animals: an insight from meta-analysis of fasting experiments. R. Soc. Open Sci. 4, 170633.
785 https://doi.org/10.1098/rsos.170633

786 Drake, J.L., Guillermic, M., Eagle, R.A., Jacobs, D.K., 2021. Fossil corals with various degrees of preservation
787 can retain information about biomineralization-related organic material. Front. Earth Sci. 9.

788 Druffel, E.R.M., 1997. Geochemistry of corals: Proxies of past ocean chemistry, ocean circulation, and climate.
789 Proc. Natl. Acad. Sci. 94, 8354–8361. https://doi.org/10.1073/pnas.94.16.8354

790 Duineveld, G.C.A., Lavaleye, M.S.S., Berghuis, E.M., 2004. Particle flux and food supply to a seamount cold-
791 water coral community (Galicia Bank, NW Spain). Mar. Ecol. Prog. Ser. 277, 13–23.
792 https://doi.org/10.3354/meps277013

793 Duineveld, G., Lavaleye, M., Bergman, M., Stigter, H., Mienis, F., 2007. Trophic structure of a cold-water coral
794 mound community (Rockall Bank, NE Atlantic) in relation to the near-bottom particle supply and current
795 regime. Bull. Mar. Sci. 81, 449–467.

796 Duineveld GCA, Jeffreys RM, Lavaleye MSS, Davies AJ, Bergman MJN, Watmough T, Witbaard R. 2012.
797 Spatial and tidal variation in food supply to shallow cold-water coral reefs of the Mingulay Reef complex
798 (Outer Hebrides, Scotland). Mar Ecol Prog Ser 444:97-115. https://doi.org/10.3354/meps09430

https://doi.org/10.5194/bg-2023-127
Preprint. Discussion started: 21 August 2023

799 Erler, D.V., Wang, X.T., Sigman, D.M., Scheffers, S.R., Shepherd, B.O., 2015. Controls on the nitrogen isotopic
800 composition of shallow water corals across a tropical reef flat transect. Coral Reefs 34, 329–338.
801 https://doi.org/10.1007/s00338-014-1215-5

802 Esri. "Ocean" [basemap]. Scale Not Given. " Ocean Basemap ". February 11, 2021.
803 https://hub.arcgis.com/maps/CESPK::ocean-basemap/explore?location=35.956244%2C-
804 111.078800%2C5.00. (December, 2022).

805 Fadlallah, Y.H., 1983. Population Dynamics and Life History of a Solitary Coral, *Balanophyllia elegans*, from
806 Central California. Oecologia 58, 200–207.

807 Fautin, D.G., 2009. Structural diversity, systematics, and evolution of cnidae. Toxicon, Cnidarian Toxins and
808 Venoms 54, 1054–1064. https://doi.org/10.1016/j.toxicon.2009.02.024

809 Fawcett, S.E., Lomas, M.W., Casey, J.R., Ward, B.B., Sigman, D.M., 2011. Assimilation of upwelled nitrate by
810 small eukaryotes in the Sargasso Sea. Nat. Geosci. 4, 717–722. https://doi.org/10.1038/ngeo1265

811 Ferrier, M.D. 1991. Net uptake of dissolved free amino acids by four scleractinian corals. *Coral Reefs* **10**, 183–
812 187. https://doi.org/10.1007/BF00336772

813 François, R., Altabet, M.A., Yu, E.-F., Sigman, D.M., Bacon, M.P., Frank, M., Bohrmann, G., Bareille, G.,
814 Labeyrie, L.D., 1997. Contribution of Southern Ocean surface-water stratification to low atmospheric
815 CO2 concentrations during the last glacial period. Nature 389, 929–935. https://doi.org/10.1038/40073

816 Freiwald, A. 2002. Reef-Forming Cold-Water Corals. In: Wefer, G., Billett, D., Hebbeln, D., Jørgensen, B.B.,
817 Schlüter, M., van Weering, T.C.E. (eds) Ocean Margin Systems. Springer, Berlin, Heidelberg.
818 https://doi.org/10.1007/978-3-662-05127-6_23

819 Ganeshram, R. S., and Pedersen, T. F. 1998, Glacial-interglacial variability in upwelling and bioproductivity off
820 NW Mexico: Implications for Quaternary paleoclimate, *Paleoceanography*, 13(6), 634– 645,
821 doi:10.1029/98PA02508.

822 Garcia-Herrera, N., Cornils, A., Laudien, J., Niehoff, B., Höfer, J., Försterra, G., González, H.E., Richter, C.,
823 2022. Seasonal and diel variations in the vertical distribution, composition, abundance and biomass of
824 zooplankton in a deep Chilean Patagonian Fjord. PeerJ 10, e12823. https://doi.org/10.7717/peerj.12823

825 Genin, A., Dayton, P.K., Lonsdale, P.F., Spiess, F.N., 1986. Corals on seamount peaks provide evidence of
826 current acceleration over deep-sea topography. Nature 322, 59–61. https://doi.org/10.1038/322059a0

827 Gonfiantini, R., W. Stichler, and K. Rosanski 1995, Standards and Intercomparison. Materials Distributed by the
828 IAEA for Stable Isotope Measurements,Int. At. Energy Agency, Vienna.

829 Goodfriend, G.A., Hare, P.E., Druffel, E.R.M. 1992. Aspartic acid racemization and protein diagenesis in corals
830 over the last 350 years. Geochim. Cosmochim. Acta 56, 3847–3850. https://doi.org/10.1016/0016-
831 7037(92)90176-J

832 Gothmann AM, Stolarski J, Adkins JF, et al. Fossil corals as an archive of secular variations in seawater
833 chemistry since the Mesozoic. *Geochim Cosmochim Acta*. 2015;160:188-208.
834 doi:https://doi.org/10.1016/j.gca.2015.03.018

835 Renaud Grover, R. Maguer, J-F, Allemand, D., Ferrier-Pagès, C. 2008. Uptake of dissolved free amino acids by
836 the scleractinian coral *Stylophora pistillata*. *J Exp Biol* 211 (6): 860–865. doi:
837 https://doi.org/10.1242/jeb.012807

838 Hannides, Cecelia C. S., Popp, Brian N., Choy, C. Anela, Drazen, Jeffrey C. 2013. Midwater zooplankton and
839 suspended particle dynamics in the North Pacific Subtropical Gyre: A stable isotope perspective,
840 *Limnology and Oceanography*, 58, doi: 10.4319/lo.2013.58.6.1931.

841 Hill, T.M., Myrvold, C.R., Spero, H.J., Guilderson, T.P. 2014. Evidence for benthic and pelagic food web
842 coupling and carbon export from California margin bamboo coral archives. *Biogeosciences* 11, 3845–
843 3854. https://doi.org/10.5194/bg-11-3845-2014

844 Hines, S.K.V., Southon, J.R., Adkins, J.F. 2015. A high-resolution record of Southern Ocean intermediate water
845 radiocarbon over the past 30,000 years. *Earth and Planetary Science Letters* 432, 46-58.
846 https://doi.org/10.1016/j.epsl.2015.09.038

847 Hoegh-Guldberg, O., Williamson, J. Availability of two forms of dissolved nitrogen to the coral Pocillopora
848 damicornis and its symbiotic zooxanthellae. *Marine Biology* **133**, 561–570 (1999).
849 https://doi.org/10.1007/s002270050496

850 Höfer, J., González, H.E., Laudien, J., Schmidt, G.M., Häussermann, V., Richter, C., 2018. All you can eat: the
851 functional response of the cold-water coral *Desmophyllum dianthus* feeding on krill and copepods. PeerJ
852 6, e5872. https://doi.org/10.7717/peerj.5872

853 Horn, M.G., Robinson, R.S., Rynearson, T.A., Sigman, D.M., 2011. Nitrogen isotopic relationship between
854 diatom-bound and bulk organic matter of cultured polar diatoms. Paleoceanography 26.
855 https://doi.org/10.1029/2010PA002080

856 Houlbrèque F, Tambutté E, Allemand D, Ferrier-Pagès C. 2004. Interactions between zooplankton feeding,
857 photosynthesis and skeletal growth in the scleractinian coral Stylophora pistillata. J Exp Biol. 4
858 Apr;207(Pt 9):1461-9. doi: 10.1242/jeb.00911. PMID: 15037640.

859 Kast, E.R., Stolper, D.A., Auderset, A., Higgins, J.A., Ren, H., Wang, X.T., Martínez-García, A., Haug, G.H.,
860 Sigman, D.M., 2019. Nitrogen isotope evidence for expanded ocean suboxia in the early Cenozoic.
861 Science 364, 386–389. https://doi.org/10.1126/science.aau5784

862 Kiriakoulakis, K., Fisher, E., Wolff, G.A., Freiwald, A., Grehan, A., Roberts, J.M., 2005. Lipids and nitrogen
863 isotopes of two deep-water corals from the North-East Atlantic: initial results and implications for their
864 nutrition, in: Freiwald, A., Roberts, J.M. (Eds.), Cold-Water Corals and Ecosystems, Erlangen Earth
865 Conference Series. Springer, Berlin, Heidelberg, pp. 715–729. https://doi.org/10.1007/3-540-27673-4_37

866 Knapp AN, DiFiore PJ, Deutsch C, Sigman DM, Lipschultz F. 2008. Nitrate isotopic composition between
867 Bermuda and Puerto Rico: Implications for N<inf>2</inf> fixation in the Atlantic Ocean. *Global*
868 *Biogeochem Cycles* 22(3). doi:10.1029/2007GB003107

869 Kuanui P, Chavanich S, Viyakarn V, Omori M, Fujita T, Lin C. 2020. Effect of light intensity on survival and
870 photosynthetic efficiency of cultured corals of different ages. *Estuar Coast Shelf Sci*. 235:106515.
871 doi:https://doi.org/10.1016/j.ecss.2019.106515

872 Knutson, D.W., Buddemeier, R.W., Smith, S.V., 1972. Coral chronometers: Seasonal growth bands in reef corals.
873 Science 177, 270–272. https://doi.org/10.1126/science.177.4045.270

https://doi.org/10.5194/bg-2023-127
Preprint. Discussion started: 21 August 2023

874 Larsson AI, Lundälv T, van Oevelen D. 2013. Skeletal growth, respiration rate and fatty acid composition in the
875 cold-water coral *Lophelia pertusa* under varying food conditions. Mar Ecol Prog Ser 483:169-184.
876 https://doi.org/10.3354/meps10284

877 Lasker, H.R., 1981. A comparison of the particulate feeding abilities of three species of Gorgonian soft coral.
878 Mar. Ecol. Prog. Ser. 5, 61–67.

879 Lewis, A.G., 1978. Concentrations of nutrients and chlorophyll on a cross-channel transect in Juan de Fuca Strait,
880 British Columbia. J. Fish. Res. Board Can. 35, 305–314. https://doi.org/10.1139/f78-055

881 Lewis, J.B., Price, W.S., 1975. Feeding mechanisms and feeding strategies of Atlantic reef corals. J. Zool. 176,
882 527–544. https://doi.org/10.1111/j.1469-7998.1975.tb03219.x

883 Lourey, M.J., Trull, T.W., Sigman, D.M., 2003. Sensitivity of δ15N of nitrate, surface suspended and deep
884 sinking particulate nitrogen to seasonal nitrate depletion in the Southern Ocean. Glob. Biogeochem.
885 Cycles 17. https://doi.org/10.1029/2002GB001973

886 Mackas, D.L., Harrison, P.J., 1997. Nitrogenous nutrient sources and sinks in the Juan de Fuca Strait/Strait of
887 Georgia/Puget Sound estuarine system: Assessing the potential for eutrophication. Estuar. Coast. Shelf
888 Sci. 44, 1–21. https://doi.org/10.1006/ecss.1996.0110

889 Maier, S.R., Bannister, R.J., van Oevelen, D., Kutti, T., 2020. Seasonal controls on the diet, metabolic activity,
890 tissue reserves and growth of the cold-water coral *Lophelia pertusa*. Coral Reefs 39, 173–187.
891 https://doi.org/10.1007/s00338-019-01886-6

892 Maier C, Hegeman J, Weinbauer MG, Gattuso J-P. Calcification of the cold-water coral *Lophelia pertusa*, under
893 ambient and reduced pH. *Biogeosciences*. 2009;6(8):1671-1680. doi:10.5194/bg-6-1671-2009

894 Maier, S.R., Kutti, T., Bannister, R.J., van Breugel, P., van Rijswijk, P., van Oevelen, D., 2019. Survival under
895 conditions of variable food availability: Resource utilization and storage in the cold-water coral *Lophelia*
896 *pertusa*. Limnol. Oceanogr. 64, 1651–1671. https://doi.org/10.1002/lno.11142

897 Marconi D, Weigand AM, Rafter PA, Matthew R. McIlvin MR, Matthew Forbes, M Casciotti, KL Sigman, DM.
898 2015. Nitrate isotope distributions on the US GEOTRACES North Atlantic cross-basin section: Signals of
899 polar nitrate sources and low latitude nitrogen cycling. *Mar Chem*. 177:143-156.
900 doi:https://doi.org/10.1016/j.marchem.2015.06.007

901 Mariotti, A., Germon, J.C., Hubert, P., Kaiser, P., Letolle, R., Tardieux, A., Tardieux, P., 1981. Experimental
902 determination of nitrogen kinetic isotope fractionation: Some principles; illustration for the
903 denitrification and nitrification processes. Plant Soil 62, 413–430. https://doi.org/10.1007/BF02374138

904 Martínez del Rio, C., Carleton, S.A., 2012. How fast and how faithful: the dynamics of isotopic incorporation
905 into animal tissues. J. Mammal. 93, 353–359. https://doi.org/10.1644/11-MAMM-S-165.1

906 McCutchan Jr, J.H., Lewis Jr, W.M., Kendall, C., McGrath, C.C., 2003. Variation in trophic shift for stable
907 isotope ratios of carbon, nitrogen, and sulfur. Oikos 102, 378–390. https://doi.org/10.1034/j.1600-
908 0706.2003.12098.x

909 McIlvin, M.R., Casciotti, K.L., 2011. Technical Updates to the Bacterial Method for Nitrate Isotopic Analyses.
910 Anal. Chem. 83, 1850–1856. https://doi.org/10.1021/ac1028984

https://doi.org/10.5194/bg-2023-127
Preprint. Discussion started: 21 August 2023

McMahon, K.W., Williams, B., Guilderson, T.P., Glynn, D.S., McCarthy, M.D., 2018. Calibrating amino acid δ13C and δ15N offsets between polyp and protein skeleton to develop proteinaceous deep-sea corals as paleoceanographic archives. Geochim. Cosmochim. Acta 220, 261–275. https://doi.org/10.1016/j.gca.2017.09.048

Middelburg, J., Mueller, C., Veuger, B. Larsson, A. I., Form, A., van Oevelen, D 2016.. Discovery of symbiotic nitrogen fixation and chemoautotrophy in cold-water corals. *Sci Rep* **5**, 17962 (2016). https://doi.org/10.1038/srep17962

Miller, M., 1995. Growth of a temperate coral: effects of temperature, light, depth, and heterotrophy. Mar. Ecol. Prog. Ser. 122, 217–225. https://doi.org/10.3354/meps122217

Minagawa, M., Wada, E., 1984. Stepwise enrichment of 15N along food chains: Further evidence and the relation between δ15N and animal age. Geochim. Cosmochim. Acta 48, 1135–1140. https://doi.org/10.1016/0016-7037(84)90204-7

Mortensen, P.B., Rapp, H.T., Båmstedt, U., 1998. Oxygen and carbon isotope ratios related to growth line patterns in skeletons of *Lophelia pertusa* (L) (Anthozoa, Scleractinia): Implications for determination of linear extension rate. Sarsia 83, 433–446. https://doi.org/10.1080/00364827.1998.10413702

Mortensen P.B., (2001) Aquarium observations on the deep-water coral *Lophelia pertusa* (L., 1758) (scleractinia) and selected associated invertebrates, Ophelia, 54:2, 83-104, DOI: 10.1080/00785236.2001.10409457

Mueller, C.E., Larsson, A.I., Veuger, B., Middelburg, J.J., van Oevelen, D., 2014. Opportunistic feeding on various organic food sources by the cold-water coral *Lophelia pertusa*. Biogeosciences 11, 123–133. https://doi.org/10.5194/bg-11-123-2014

Murray, J.W., Roberts, E., Howard, E., O'Donnell, M., Bantam, C., Carrington, E., Foy, M., Paul, B., Fay, A., 2015. An inland sea high nitrate-low chlorophyll (HNLC) region with naturally high pCO2. Limnol. Oceanogr. 60, 957–966. https://doi.org/10.1002/lno.10062

Muscatine, L., Goiran, C., Land, L., Jaubert, J., Cuif, J.-P., Allemand, D., 2005. Stable isotopes (δ13C and δ15N) of organic matrix from coral skeleton. Proc. Natl. Acad. Sci. 102, 1525–1530. https://doi.org/10.1073/pnas.0408921102

Naumann, M.S., Orejas, C., Wild, C., Ferrier-Pagès, C., 2011. First evidence for zooplankton feeding sustaining key physiological processes in a scleractinian cold-water coral. J. Exp. Biol. 214, 3570–3576. https://doi.org/10.1242/jeb.061390

Naumann, M.S., Tolosa, I., Taviani, M., Grover, R., Ferrier-Pagès, C., 2015. Trophic ecology of two cold-water coral species from the Mediterranean Sea revealed by lipid biomarkers and compound-specific isotope analyses. Coral Reefs 34, 1165–1175. https://doi.org/10.1007/s00338-015-1325-8

Orejas C, Ferrier-Pagès C, Reynaud S, Tsounis G, Allemand D, Gili JM. 2011. Experimental comparison of skeletal growth rates in the cold-water coral *Madrepora oculata* Linnaeus, 1758 and three tropical scleractinian corals. *J Exp Mar Bio Ecol*. 2011;405(1):1-5. doi:https://doi.org/10.1016/j.jembe.2011.05.008

Orejas C, Ferrier-Pagès C, Reynaud S, Gori A and others. 2011. Long-term growth rates of four Mediterranean cold-water coral species maintained in aquaria. Mar Ecol Prog Ser 429:57-65. https://doi.org/10.3354/meps09104

https://doi.org/10.5194/bg-2023-127
Preprint. Discussion started: 21 August 2023

950 Osinga, R., Schutter, M., Griffioen, B. *et al.* 2011. The Biology and Economics of Coral Growth. *Mar Biotechnol*
951 **13**, 658–671 (2011). https://doi.org/10.1007/s10126-011-9382-7

952 Pride C, Thunell R, Sigman D, Keigwin L, Altabet M, Tappa E. 1999. Nitrogen isotopic variations in the Gulf of
953 California since the Last Deglaciation: Response to global climate change. *Paleoceanography* 14(3).
954 doi:10.1029/1999PA900004

955 Purser A, Larsson AI, Thomsen L, van Oevelen D. 2010. The influence of flow velocity and food concentration
956 on *Lophelia pertusa* (Scleractinia) zooplankton capture rates. *J Exp Mar Bio Ecol*. 395(1):55-62.
957 doi:https://doi.org/10.1016/j.jembe.2010.08.013

958 Rae, J.W.B. 2018. Boron Isotopes in Foraminifera: Systematics, Biomineralisation, and CO_2 Reconstruction. In:
959 Marschall, H., Foster, G. (eds) Boron Isotopes. Advances in Isotope Geochemistry. Springer, Cham.
960 https://doi.org/10.1007/978-3-319-64666-4_5

961 Rangel, M.S., Erler, D., Tagliafico, A., Cowden, K., Scheffers, S., Christidis, L., 2019. Quantifying the transfer
962 of prey δ15N signatures into coral holobiont nitrogen pools. Mar. Ecol. Prog. Ser. 610, 33–49.
963 https://doi.org/10.3354/meps12847

964 Ren, H., Chen, Y.-C., Wang, X.T., Wong, G.T.F., Cohen, A.L., DeCarlo, T.M., Weigand, M.A., Mii, H.-S.,
965 Sigman, D.M., 2017. 21st-century rise in anthropogenic nitrogen deposition on a remote coral reef.
966 Science 356, 749–752. https://doi.org/10.1126/science.aal3869

967 Reynaud, S., Martinez, P., Houlbrèque, F., Billy, I., Allemand, D., Ferrier-Pagès, C., 2009. Effect of light and
968 feeding on the nitrogen isotopic composition of a zooxanthellate coral: role of nitrogen recycling. Mar.
969 Ecol. Prog. Ser. 392, 103–110. https://doi.org/10.3354/meps08195

970 Roberts, J.M., Wheeler, A.J., Freiwald, A., 2006. Reefs of the deep: The biology and geology of cold-water coral
971 ecosystems. Science 312, 543–547. https://doi.org/10.1126/science.1119861

972 Robinson, R.S., Kienast, M., Albuquerque, A.L., Altabet, M., Contreras, S., Holz, R.D.P., Dubois, N., Francois,
973 R., Galbraith, E., Hsu, T.-C., Ivanochko, T., Jaccard, S., Kao, S.-J., Kiefer, T., Kienast, S., Lehmann, M.,
974 Martinez, P., McCarthy, M., Möbius, J., Pedersen, T., Quan, T.M., Ryabenko, E., Schmittner, A.,
975 Schneider, R., Schneider-Mor, A., Shigemitsu, M., Sinclair, D., Somes, C., Studer, A., Thunell, R., Yang,
976 J.-Y., 2012. A review of nitrogen isotopic alteration in marine sediments. Paleoceanography 27.
977 https://doi.org/10.1029/2012PA002321

978 Robinson LF, Adkins JF, Frank N, Gagnon, A.C., Prouty, N.G., Roark, B. van de Flierdt, T. 2014. The
979 geochemistry of deep-sea coral skeletons: A review of vital effects and applications for
980 palaeoceanography. *Deep Sea Res Part II Top Stud Oceanogr*. 99:184-198.
981 doi:https://doi.org/10.1016/j.dsr2.2013.06.005

982 Robinson RS, Sigman DM. 2008. Nitrogen isotopic evidence for a poleward decrease in surface nitrate within the
983 ice age Antarctic. *Quat Sci Rev*. 27(9-10). doi:10.1016/j.quascirev.2008.02.005

984 Robinson, R.S., Smart, S.M., Cybulski, J.D., McMahon, K.W., Marcks, B., Nowakowski, C., 2023. Insights from
985 fossil-bound nitrogen isotopes in diatoms, foraminifera, and corals. Annu. Rev. Mar. Sci. 15, null.
986 https://doi.org/10.1146/annurev-marine-032122-104001

https://doi.org/10.5194/bg-2023-127
Preprint. Discussion started: 21 August 2023

987 Saino, T., Hattori, A., 1987. Geographical variation of the water column distribution of suspended particulate
988 organic nitrogen and its 15N natural abundance in the Pacific and its marginal seas. Deep Sea Res. A 34,
989 807–827. https://doi.org/10.1016/0198-0149(87)90038-0

990 Scrimgeour, C.M., Gordon, S.C., Handley, L.L., Woodford, J.A.T., 1995. Trophic levels and anomalous δ15N of
991 insects on raspberry (Rubus Idaeus L.). Isotopes Environ. Health Stud. 31, 107–115.
992 https://doi.org/10.1080/10256019508036256

993 Sebens, K.P., Vandersall, K.S., Savina, L.A., Graham, K.R., 1996. Zooplankton capture by two scleractinian
994 corals, Madracis mirabilis andMontastrea cavernosa, in a field enclosure. Mar. Biol. 127, 303–317.
995 https://doi.org/10.1007/BF00942116

996 Sherwood, O.A., Heikoop, J.M., Scott, D.B., Risk, M.J., Guilderson, T.P., McKinney, R.A., 2005. Stable isotopic
997 composition of deep-sea gorgonian corals *Primnoa* spp.: a new archive of surface processes. Mar. Ecol.
998 Prog. Ser. 301, 135–148. https://doi.org/10.3354/meps301135

999 Sherwood, O.A., Jamieson, R.E., Edinger, E.N., Wareham, V.E., 2008. Stable C and N isotopic composition of
000 cold-water corals from the Newfoundland and Labrador continental slope: Examination of trophic, depth
001 and spatial effects. Deep Sea Res. Part Oceanogr. Res. Pap. 55, 1392–1402.
002 https://doi.org/10.1016/j.dsr.2008.05.013

003 Sherwood, O.A., Thresher, R.E., Fallon, S.J., Davies, D.M., Trull, T.W., 2009. Multi-century time-series of ^{15}N
004 and ^{14}C in bamboo corals from deep Tasmanian seamounts: evidence for stable oceanographic
005 conditions. Mar. Ecol. Prog. Ser. 397, 209–218. https://doi.org/10.3354/meps08166

006 Schutter, M., Crocker, J., Paijmans, A., Janse, M., Osinga, R. Verreth, J.A.J., Wijffels, R.H. 2010. The effect of
007 different flow regimes on the growth and metabolic rates of the scleractinian coral *Galaxea fascicularis* .
008 *Coral Reefs* **29**, 737–748. https://doi.org/10.1007/s00338-010-0617-2

009 Sigman, D.M., Altabet, M.A., McCorkle, D.C., Francois, R., Fischer, G., 1999. The $\delta^{15}N$ of nitrate in the
010 Southern Ocean: Consumption of nitrate in surface waters. Glob. Biogeochem. Cycles 13, 1149–1166.
011 https://doi.org/10.1029/1999GB900038

012 Sigman, D., Boyle, E. Glacial/interglacial variations in atmospheric carbon dioxide. 2000. *Nature* **407**, 859–869
013 (2000). https://doi.org/10.1038/35038000

014 Sigman, D.M., Casciotti, K.L., Andreani, M., Barford, C., Galanter, M., Böhlke, J.K., 2001. A Bacterial method
015 for the nitrogen isotopic analysis of nitrate in seawater and freshwater. Anal. Chem. 73, 4145–4153.
016 https://doi.org/10.1021/ac010088e

017 Sigman, D.M., Fripiat, F., 2019. *Nitrogen Isotopes in the Ocean*, in: Cochran, J.K., Bokuniewicz, H.J., Yager,
018 P.L. (Eds.), Encyclopedia of Ocean Sciences (Third Edition). Academic Press, Oxford, pp. 263–278.
019 https://doi.org/10.1016/B978-0-12-409548-9.11605-7

020 Soetaert, K., Mohn, C., Rengstorf, A., Grehan, A., van Oevelen, D., 2016. Ecosystem engineering creates a direct
021 nutritional link between 600-m deep cold-water coral mounds and surface productivity. Sci. Rep. 6,
022 35057. https://doi.org/10.1038/srep35057

023 Spero, H.J., Andreasen, D.J., Sorgeloos, P., 1993. Carbon and nitrogen isotopic composition of different strains
024 of *Artemia* sp. Int. J. Salt Lake Res. 2, 133. https://doi.org/10.1007/BF02905905

https://doi.org/10.5194/bg-2023-127
Preprint. Discussion started: 21 August 2023

025 Tanaka, Y., Miyajima, T., Koike, I., Hayashibara, T., Ogawa, H., 2006. Translocation and conservation of
026 organic nitrogen within the coral-zooxanthella symbiotic system of Acropora pulchra, as demonstrated
027 by dual isotope-labeling techniques. J. Exp. Mar. Biol. Ecol. 336, 110–119.
028 https://doi.org/10.1016/j.jembe.2006.04.011

029 Tanaka, Y., Suzuki, A., Sakai, K., 2018. The stoichiometry of coral-dinoflagellate symbiosis: carbon and nitrogen
030 cycles are balanced in the recycling and double translocation system. ISME J. 12, 860–868.
031 https://doi.org/10.1038/s41396-017-0019-3

032 Teece, M.A., Estes, B., Gelsleichter, E., Lirman, D., 2011. Heterotrophic and autotrophic assimilation of fatty
033 acids by two scleractinian corals, Montastraea faveolata and Porites astreoides. Limnol. Oceanogr. 56,
034 1285–1296. https://doi.org/10.4319/lo.2011.56.4.1285

035 Thiagarajan N., Subhas A. V., Southon J. R., Eiler J. M. andAdkins J. F. 2014. Abrupt pre-Bolling-Allerod
036 warming and circulation changes in the deep ocean. Nature 511, 75–78.
037 https://doi.org/10.1038/nature13472

038 Thiem, Ø., Ravagnan, E., Fosså, J.H., Berntsen, J., 2006. Food supply mechanisms for cold-water corals along a
039 continental shelf edge. J. Mar. Syst. 60, 207–219. https://doi.org/10.1016/j.jmarsys.2005.12.004

040 Thomas, S.M., Crowther, T.W., 2015. Predicting rates of isotopic turnover across the animal kingdom: a
041 synthesis of existing data. J. Anim. Ecol. 84, 861–870. https://doi.org/10.1111/1365-2656.12326

042 Treibergs, L.A., Fawcett, S.E., Lomas, M.W., Sigman, D.M., 2014. Nitrogen isotopic response of prokaryotic and
043 eukaryotic phytoplankton to nitrate availability in Sargasso Sea surface waters. Limnol. Oceanogr. 59,
044 972–985. https://doi.org/10.4319/lo.2014.59.3.0972

045 Tsounis G, Orejas C, Reynaud S, JM G, Allemand D, Ferrier-Pagès C. 2010. Prey-capture rates in four
046 Mediterranean cold water corals . *Mar Ecol Prog Ser*. 398:149-155. https://doi.org/10.3354/meps08312

047 van Oevelen, P., Duineveld, G., Lavaleye, M., Mienis, Furu, Soetaert, Karline, H., Carlo H. R., 2009. The cold-
048 water coral community as hotspot of carbon cycling on continental margins: A food-web analysis from
049 Rockall Bank (northeast Atlantic), *Limnology and Oceanography*, 54, doi: 10.4319/lo.2009.54.6.1829.

050 Vinogradov, M. E. Feeding of the deep-sea zooplankton. 1962. *Rapp. Pv. Reun. Cons. Perm. Int. Exp. Mer.* **153**,
051 114–120.

052 Wang, X.T., Prokopenko, M.G., Sigman, D.M., Adkins, J.F., Robinson, L.F., Ren, H., Oleynik, S., Williams, B.,
053 Haug, G.H., 2014. Isotopic composition of carbonate-bound organic nitrogen in deep-sea scleractinian
054 corals: A new window into past biogeochemical change. Earth Planet. Sci. Lett. 400, 243–250.
055 https://doi.org/10.1016/j.epsl.2014.05.048

056 Wang, X.T., Sigman, D.M., Prokopenko, M.G., Adkins, J.F., Robinson, L.F., Hines, S.K., Chai, J., Studer, A.S.,
057 Martínez-García, A., Chen, T., Haug, G.H., 2017. Deep-sea coral evidence for lower Southern Ocean
058 surface nitrate concentrations during the last ice age. Proc. Natl. Acad. Sci. 114, 3352–3357.
059 https://doi.org/10.1073/pnas.1615718114

060 Webb, S., Hedges, R., Simpson, S., 1998. Diet quality influences the $\delta^{13}C$ and $\delta^{15}N$ of locusts and their
061 biochemical components. J. Exp. Biol. 201, 2903–2911. https://doi.org/10.1242/jeb.201.20.2903

https://doi.org/10.5194/bg-2023-127
Preprint. Discussion started: 21 August 2023

062 Weigand, M.A., Foriel, J., Barnett, B., Oleynik, S., Sigman, D.M., 2016. Updates to instrumentation and
063 protocols for isotopic analysis of nitrate by the denitrifier method. Rapid Commun. Mass Spectrom. 30,
064 1365–1383. https://doi.org/10.1002/rcm.7570

065 Williams, B., and Grottoli, A. G. 2010. Recent shoaling of the nutricline and thermocline in the western tropical
066 Pacific, *Geophys. Res. Lett.*, 37, L22601, doi:10.1029/2010GL044867.

067 Wishner, K.F., Meise-Munns, C.J., 1984. In situ grazing rates of deep-sea benthic boundary-layer zooplankton.
068 Mar. Biol. 84, 65–74. https://doi.org/10.1007/BF00394528

069 Zhou, M., Granger, J., Chang, B.X., 2022. Influence of sample volume on nitrate N and O isotope ratio analyses
070 with the denitrifier method. Rapid Commun. Mass Spectrom. 36, e9224.
071 https://doi.org/10.1002/rcm.9224